AQUIFER RECHARGE ESTIMATES BASED ON UNSATURATED ZONE

MEASUREMENTS, NEW JERSEY

A Draft Thesis

Presented to

The Faculty of the Department of Geology

San Jose State University

In Partial Fulfillment

of the Requirements for the Degree

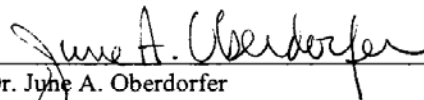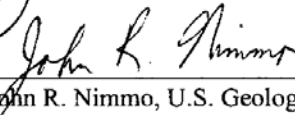Master of Science

by

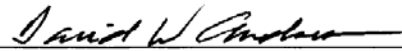Kimberlie S. Perkins

August 2005

APPROVED FOR THE DEPARTMENT OF GEOLGY

Dr. June A. Oberdorfer

Dr. John R. Nimmo, U.S. Geological Survey

Dr. David W. Andersen

APPROVED FOR THE UNIVERSITY

ABSTRACT

AQUIFER RECHARGE ESTIMATES BASED ON UNSATURATED ZONE

MEASUREMENTS, NEW JERSEY

By Kimberlie S. Perkins

Aquifer recharge was estimated for six locations in southern New Jersey. The Darcian method was used with unsaturated zone sediment properties that were measured directly and predicted by multiple methods. This study shows that estimated recharge rates can be highly variable depending on the chosen technique. Measured hydraulic properties yielded reasonable recharge rates, although interpolation of measured data proved critical. Errors in measured field water contents required by the Darcian method also had a large effect on predicted recharge rates. Very slight variations in field water content values can translate into order-of-magnitude differences in estimated recharge rates due to the highly nonlinear relationship between hydraulic conductivity and water content. While episodic recharge was observed in a uniform soil, significant layering appears to slow downward flow. This results in a more diffuse, less pulse-like wetting front and, therefore, less variable recharge over time.

ACKNOWLEDGEMENTS

TABLE OF CONTENTS

LIST OF ILLUSTRATIONS

LIST OF TABLES

INTRODUCTION

Understanding the nature of recharge to the Kirkwood-Cohansey aquifer system
(Fig. 1) is fundamental to understanding the relationship between ground water quality
and land use in the southern New Jersey coastal plain region. Several water-budget
studies have been done by the United States Geological Survey (USGS) to estimate
aquifer recharge in southern New Jersey; however, there is a need to evaluate recharge
rates and processes on a more localized scale. Published annual recharge estimates range
from 33 to 49 cm/yr (Watt and Johnson, 1992; Watt and others, 1994; Johnson and Watt,
1994; Johnson and Charles, 1997; Charles and others, 2001). This study aims to evaluate
recharge rates and processes at the local scale and is complementary to a larger project
within the USGS Glassboro study area in southern New Jersey (Fig. 2) designed to: (1)
examine spatial variability of aquifer recharge, (2) evaluate possible causes of variability,
and (3) identify areas of potential risk of environmental damage, for example, those areas
with high recharge occurring where agricultural contamination may be an issue.

In the study presented here, using water budget recharge estimates (Watt and
Johnson, 1992; Watt and others, 1994; Johnson and Watt, 1994; Johnson and Charles,
1997; Charles and others, 2001) as a gauge of reasonable values and annual precipitation
as an upper limit, several variations on a Darcy's law-based recharge estimation
technique were compared to determine which may be appropriate for recharge estimation
in the coastal plain environment. Unsaturated hydraulic properties were measured in the
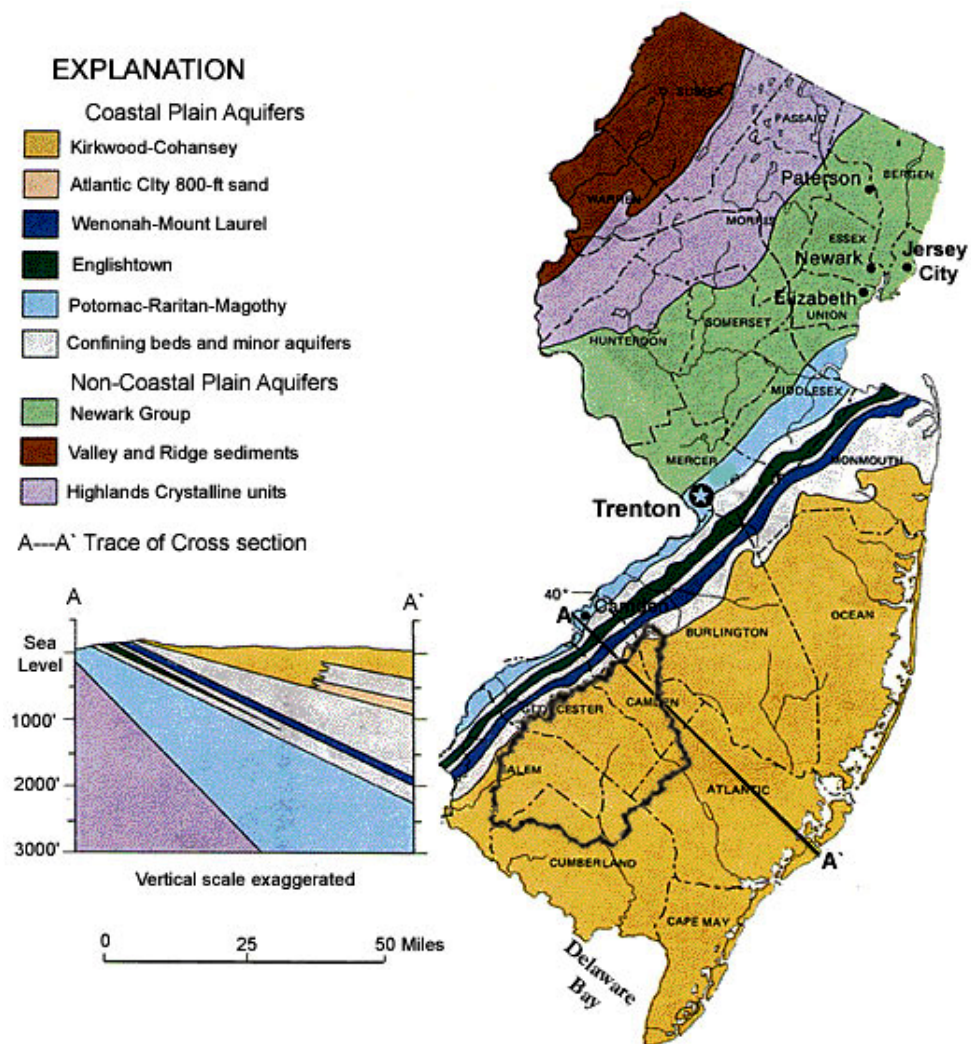
Figure 1. Principal aquifers of New Jersey. The Glassboro study site (outlined in black) is located within the region of the Kirkwood-Cohansey aquifer (modified from Zapecza, 1989).
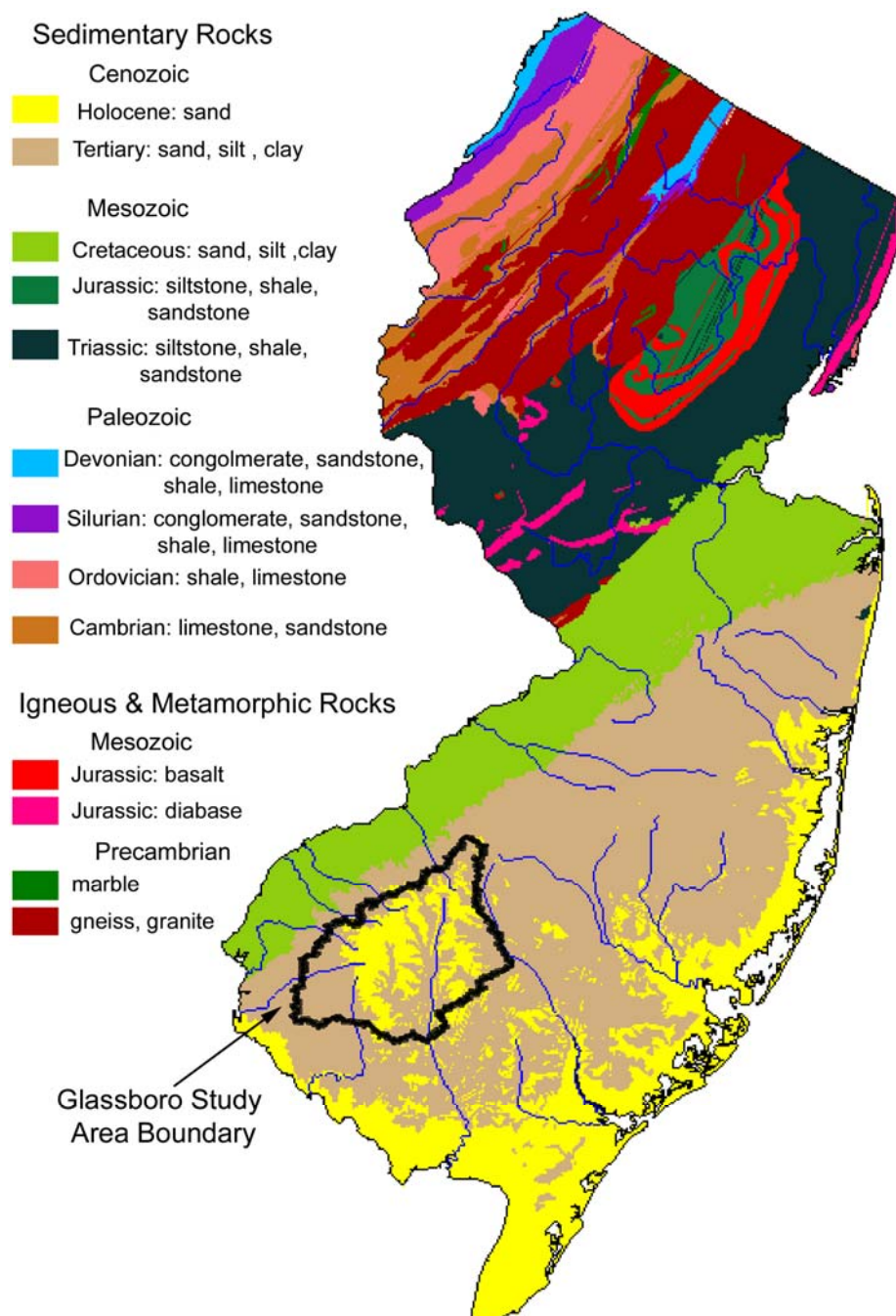
Figure 2. Geologic map of New Jersey including the location of Glassboro study area (modified from Zapecza, 1989).

laboratory and treated with various fitting and parameterization techniques for Darcian recharge estimation. Because unsaturated hydraulic properties are costly and time consuming to measure, models that estimate these properties without direct measurement were also evaluated in this study. The unsaturated zone at this site, as in many coastal plain regions, is mainly sand to sandy loam in texture, which is considered a highly favorable case for soil hydraulic property estimation. Water table fluctuations were also used for comparison to Darcian-estimated recharge rates. Numerical computer simulations were run to evaluate the existence of steady-state flow in the unsaturated zone at one site.

Focusing on six locations (Fig. 3), the main goals of this study were to evaluate the nature of flow through the unsaturated zone and to determine which method or methods may be appropriate for point recharge estimation in this coastal plain environment. The methods used in this study include recharge estimation based on (1) measured unsaturated hydraulic conductivity with several types of curve fitting techniques, (2) estimated unsaturated hydraulic conductivity from the Arya-Paris model (Arya and Paris, 1981) and van Genuchten-Mualem model (van Genuchten, 1980) in combination, (3) estimated unsaturated hydraulic conductivity from the Rosetta pedotransfer function model (U.S. Department of Agriculture, 2001), and (4) the water table fluctuation method. Finite difference unsaturated flow modeling with measured and estimated hydraulic properties was also used to evaluate the assumption of steady flow at one of the sites. Results from the various techniques were evaluated individually and compared to examine the utility and deficiencies of each method.
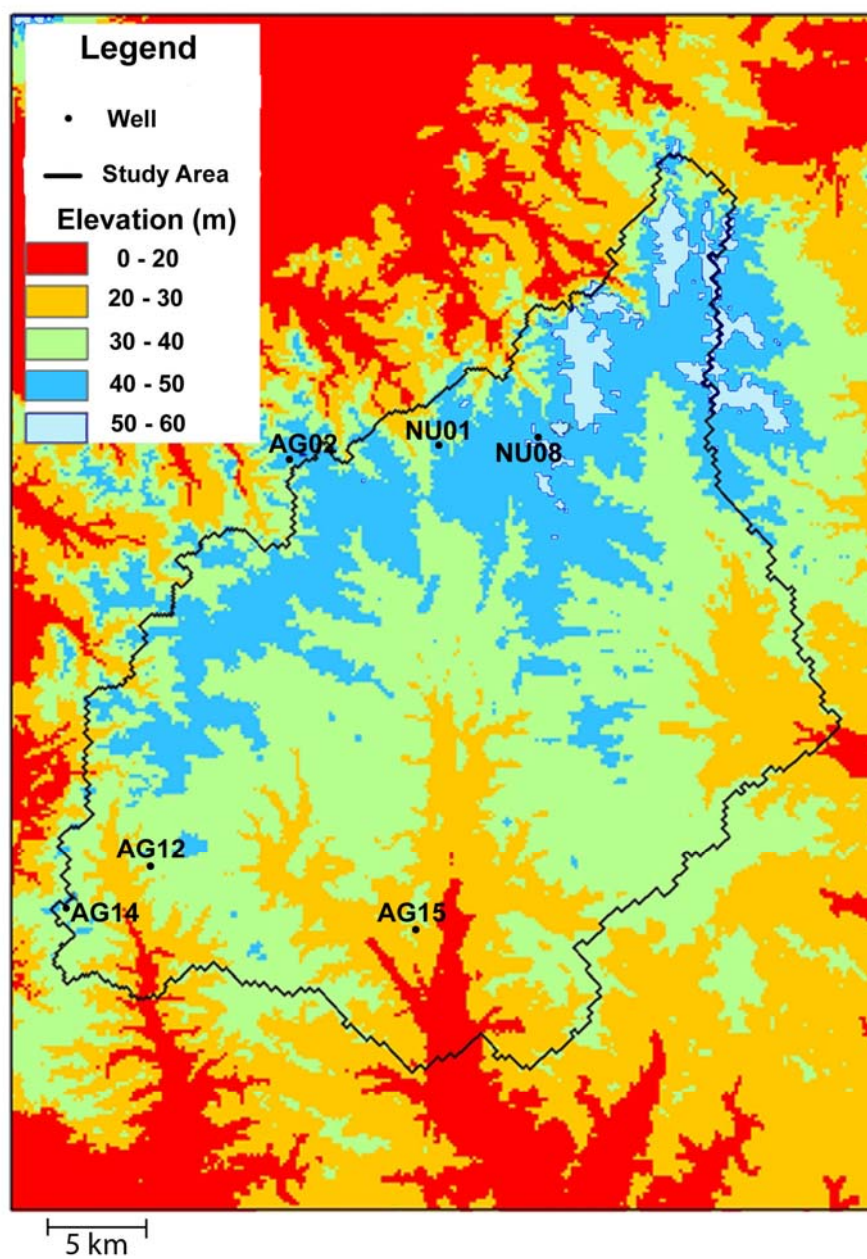
Figure 3. Digital elevation map (Kauffman, 2002, personal communication) showing locations where samples were collected for hydraulic property measurements.

SITE DESCRIPTION

The Glassboro study area comprises about 930 km^2 within the New Jersey Coastal Plain province. The population within the study area, which has a mix of urban and agricultural land use, has steadily risen from about 50,000 in 1940 to 250,000 in 2000 (Baehr and others, 2002). The volume of water pumped from the Kirkwood-Cohansey aquifer system has also increased along with suburban growth. More than 75 percent of the public freshwater supply in the region comes from high-capacity production wells that commonly yield 1890 to 3790 L per minute (500 to 1,000 gallons per minute), with many exceeding 3790 L per minute (U.S. Geological Survey, 1998).

The Kirkwood-Cohansey aquifer (Fig. 1) within the study area is approximately 35 m thick and consists of highly permeable sand with some silt and clay. The hydrologic importance of this aquifer system is not only its high yield, but also its ability to replenish lower water-bearing units and influence contaminant transport. An outcrop of the Kirkwood Formation, a confining unit about 30 m thick, forms the northwest boundary of the study area and underlies the unconsolidated Kirkwood-Cohansey aquifer, which thickens in the southeast (Zapecza, 1989). Most of the sediment in the unsaturated zone is composed of the Cohansey sand unit, which was deposited during the Miocene (Fig. 1). The Cohansey sand unit consists of inner shelf, nearshore, and beach deposits that developed during oceanic retreat. The sand generally coarsens upward, as do similarly deposited formations of the New Jersey Coastal Plain (Zapecza, 1989).

Average annual precipitation for the study area is about 109.4 cm, of which 25.4, 29.1, 29.1, and 25.8 cm are apportioned during the winter, spring, summer, and fall seasons, respectively (Baehr and others, 2002). Figure 4 shows monthly precipitation records for the period of 1994 through spring of 2000 from the National Oceanic and Atmospheric Administration's Glassboro 2 weather station (ID 283291). Although precipitation is nearly evenly distributed throughout the year, the average daily seasonal temperatures, 0.8, 11.1, 23.2, 13.7 ^{o}C for winter, spring, summer, and fall seasons, respectively, contribute to the variability in the average seasonal potential evapotranspiration (ET). ET values as calculated by the Thornthwaite method (Thornthwaite and Mather, 1957) are 0.7, 14.9, 41.5, and 16.2 cm, for winter, spring, summer, and fall seasons respectively (Baehr and others, 2002).
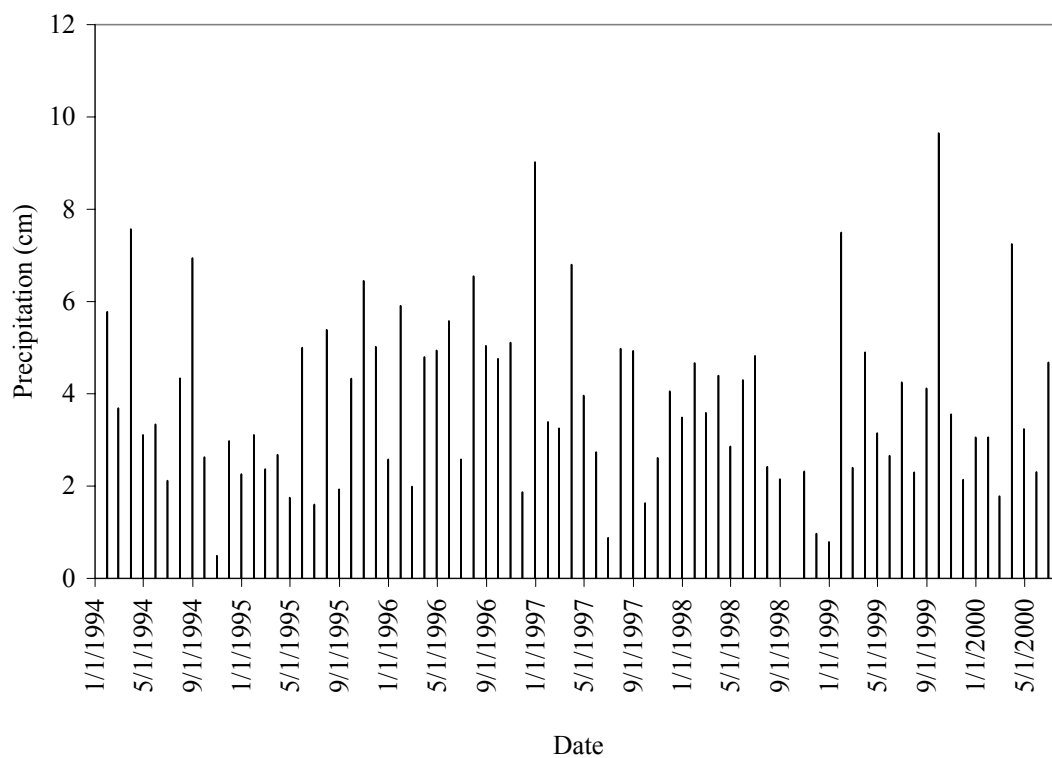
Figure 4. Monthly precipitation data from the National Oceanic and Atmospheric Administration's Glassboro 2 weather station (ID 283291)from January 1994 through June 2000 (Baehr, 2002, personal communication).

BACKGROUND

Between July 30 and October 24 of 1996, the U.S. Geological Survey installed 48 observation wells in the Kirkwood-Cohansey aquifer system in southern New Jersey within the Glassboro study area (Baehr and others, 2002). This allowed for collection of unsaturated-zone sediment and measurement of depth-dependent, gravimetrically-determined water content at the 48 locations to be used in estimating the spatial variability of recharge over the region. Gravimetric water contents were determined by weighing core samples directly after collection and weighing again after subsequent oven drying (Gardner, 1986). Errors in gravimetric field-water contents determined by conducting measurements on replicate core samples from the same depths were approximately +/-10 percent (Baehr, 2002, personal communication).

Some of the profiles of water content vs. depth appeared to have possible zones of steady flow at the time of sampling, suggesting that the Darcian steady-state centrifuge (SSC) method (Nimmo and others, 1994) could be applied to estimate recharge rates. If water content is unchanging in time at a depth below which evapotranspiration and other surface condition effects are damped out, it is possible that unsaturated flow and hence recharge rates are steady and driven by gravity alone. Six locations were chosen for unsaturated hydraulic property measurements on core samples taken from zones where the water-content profiles appeared to be steadiest. Three of the locations are in the north end of the Glassboro study area and three are in the south (Fig. 3).

For the study presented here, the sites were categorized based on water-content profiles measured during different seasons. Two of the sites, AG-02 and AG-14 appeared to have steady flow at depth year-round (Fig. 5), two of the sites, AG-12 and NU-08, appeared to have seasonally steady flow where water content is the same in a given season over time (Fig. 6), and two of the sites, AG-15 and NU-01 did not exhibit steady flow conditions (Fig. 7). Table 1 contains sediment descriptions for each site based on sampling notes and particle-size distributions measured on bulk and core samples. Some layers were defined solely on sediment description or particle-size distribution, and some layers were defined on both where possible.

Because the SSC measurements are costly and time consuming, particle-size distributions were also measured on 109 bulk samples in order to assess the spatial variability of recharge over the entire study area using a model based on textural data (Baehr and others, 2002). The Rosetta model (U.S. Department of Agriculture, 2001), which requires only textural and bulk-density data, was used by Baehr and others (2002) to estimate hydraulic properties and ultimately recharge over the entire region. Though the recharge rates calculated for all 48 locations varied greatly, median recharge calculated for the surficial Kirkwood-Cohansey aquifer by Baehr and others (2002) was 29.2 cm/yr, which compares favorably to estimates from water budget studies (Watt and Johnson, 1992; Watt and others, 1994; Johnson and Watt, 1997; Johnson and Charles, 1997; Charles and others, 2001). Spatially distributed recharge rates were interpolated by kriging and mapped over the study area to evaluate variability patterns. Because many of the estimated values were unreasonable (for example recharge rates much higher than
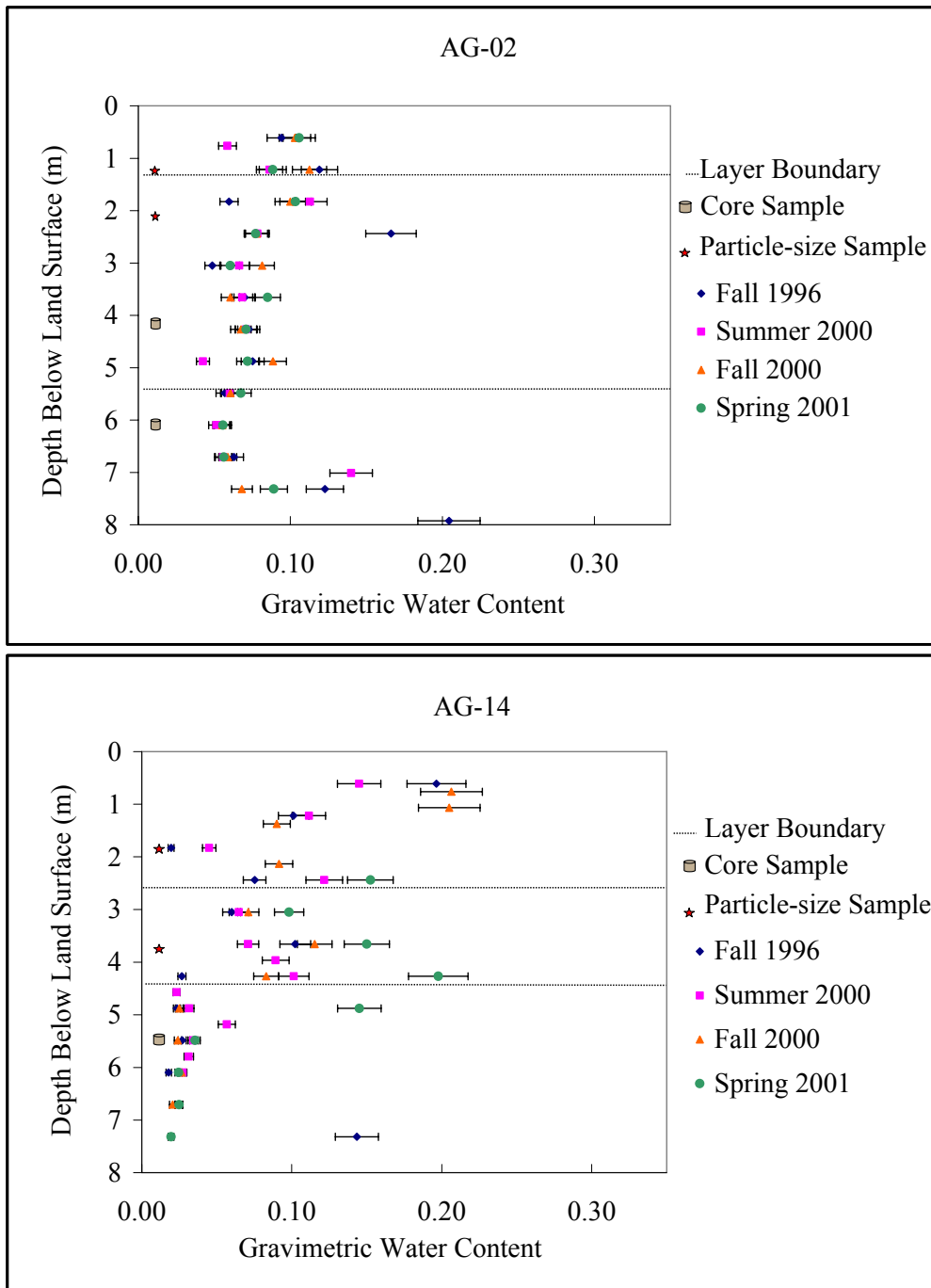
Figure 5. Profiles of water content at various times for sites AG-02 and AG-14 (Baehr, 2002, personal communication). Core samples were taken as indicated from the zones that appeared relatively steady. Bulk samples were taken for particle-size analysis as indicated to evaluate heterogeneity and define layers along with lithology logs. Error bars indicate +/- 10% error in determination of field water content.
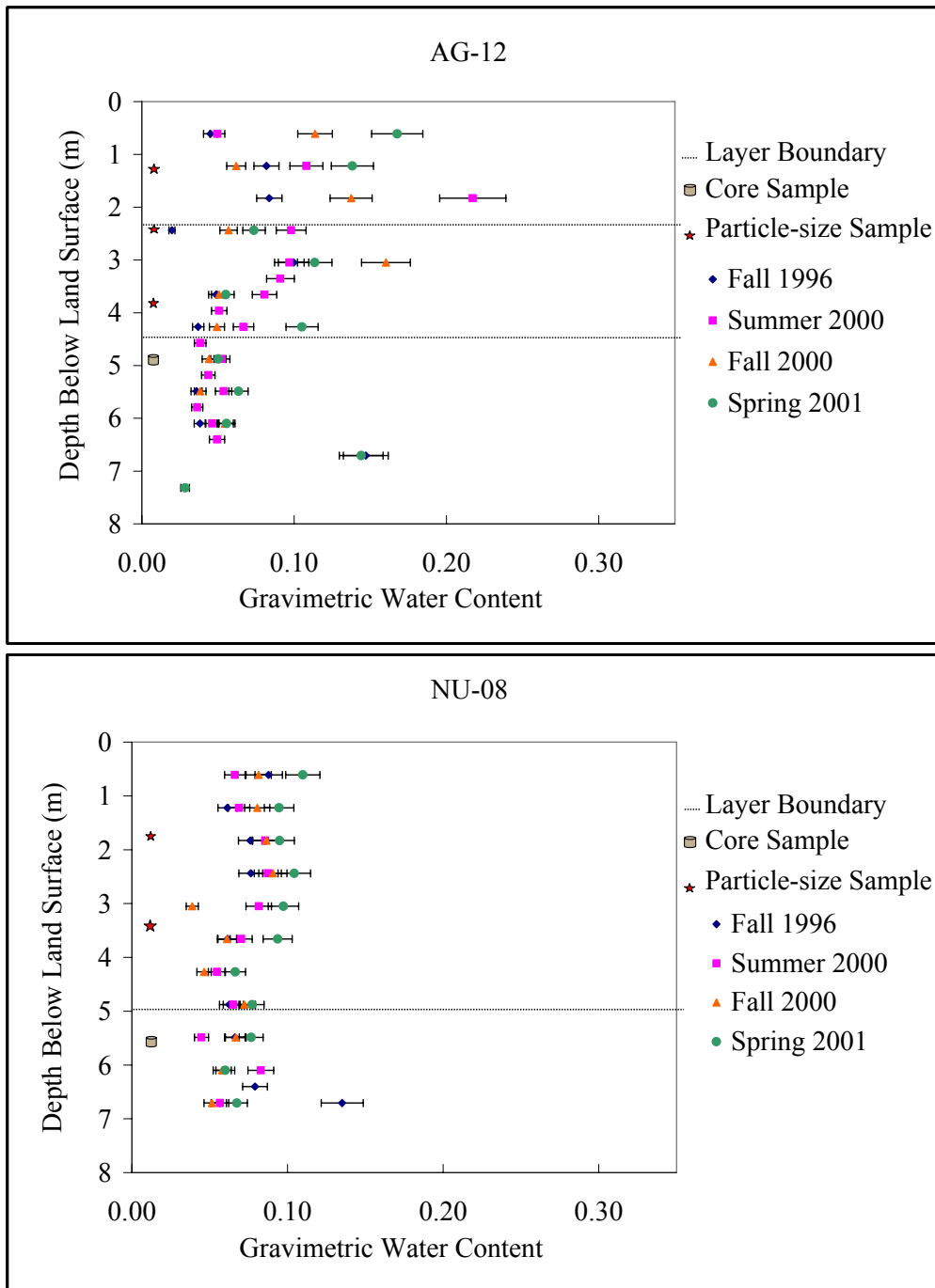
Figure 6. Profiles of water content at various times for sites AG-12 and NU-08 (Baehr, 2002, personal communication). Core samples were taken as indicated from the zones that appeared seasonally steady. Bulk samples were taken for particle-size analysis to evaluate heterogeneity and define layers along with lithology logs. Error bars indicate +/- 10% error in determination of field water content.
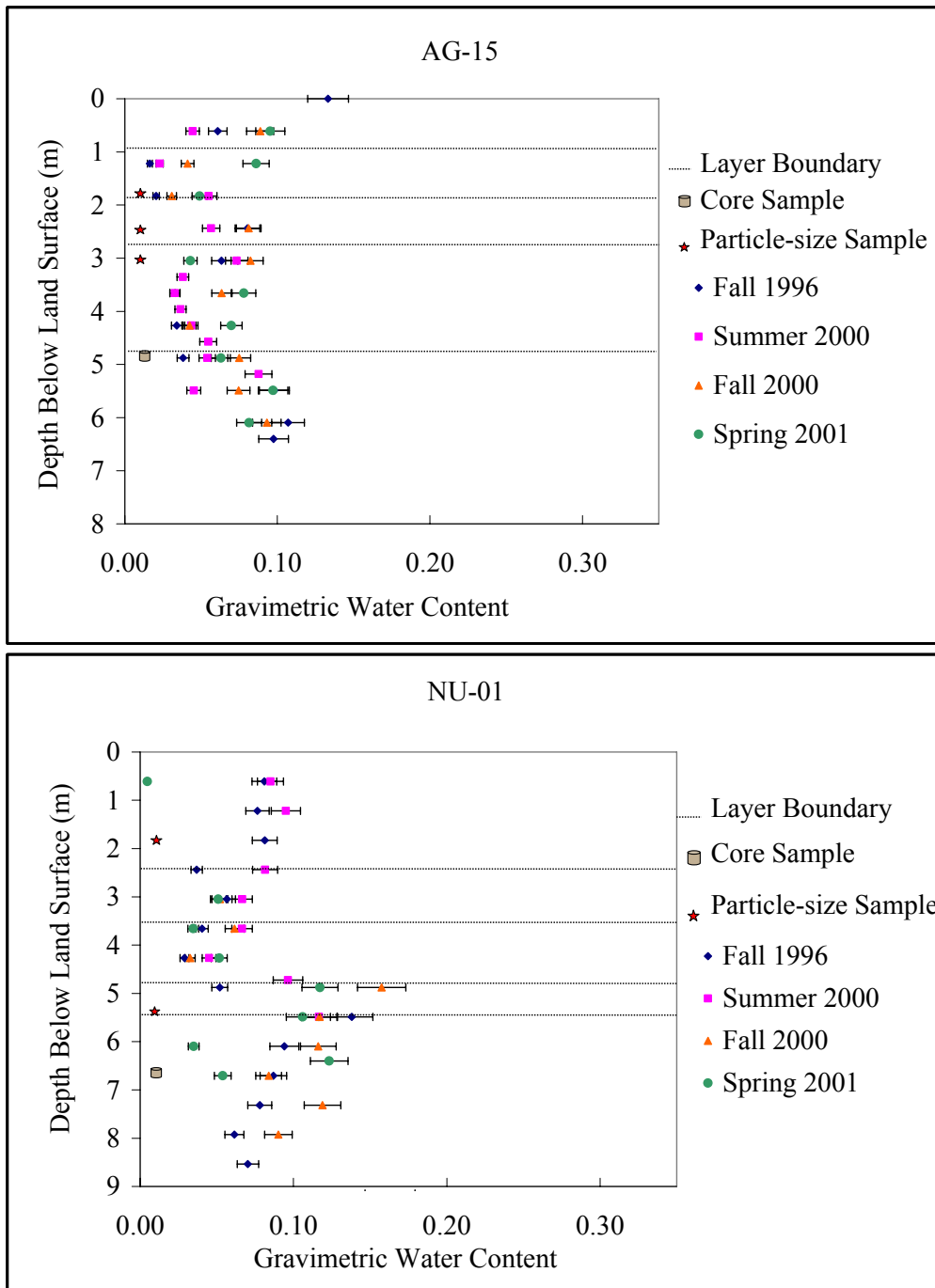
Figure 7. Profiles of water content at various times for sites AG-15 and NU-01 (Baehr, 2002, personal communication). Core and bulk samples were taken to evaluate heterogeneity and define layers along with lithology logs. Error bars indicate +/- 10% error in determination of field water content.

Table 1. Unsaturated zone sediment characteristics based on sampling logs and/or measured particle size distributions.

Site	Depth interval	Description
AG-02	0-1.2 m 1.2-5.5 m 5.5-7.6 m	Coarse sand and gravel Fine sand with some gravel Coarse sand, little gravel
AG-14	0-2.6 m 2.6-4.3 m 4.3-10.4 m	Medium sand and gravel Sand and silt Coarse sand
AG-12	0-1.8 m 1.8-4.5 m 4.5-11.9	Medium sand, silt, and gravel Medium-coarse sand, little gravel Medium sand
NU-08	0-5.0 m 5.0-9.1 m	Medium sand with some gravel Medium sand
AG-15	0-0.9 m 0.9-1.8 m 1.8-2.7 m 2.7-4.9 m 4.9-8.8 m	Fine sand and clay Medium sand Medium sand and gravel Fine-medium sand and gravel Medium sand
NU-01	0-2.6 m 2.6-3.4 m 3.4-4.9 m 4.9-5.5 m 5.5-12.2 m	Medium sand and gravel Fine sand Fine-medium sand Fine sand with little gravel Medium sand with little gravel

rainfall), they were used only to statistically rank recharge areas into broad categories such as higher or lower than the average rate (Fig. 8). The resulting map revealed a low-recharge, largely agricultural part of the study area where recharge was previously found to be low relative to other basins (Baehr and others, 2002). The study presented here focuses only on the six locations within the Glassboro study area for which hydraulic properties were measured (Fig. 3) and aims to assess steadiness of flow and values of recharge predicted by different methods at those particular points in space.
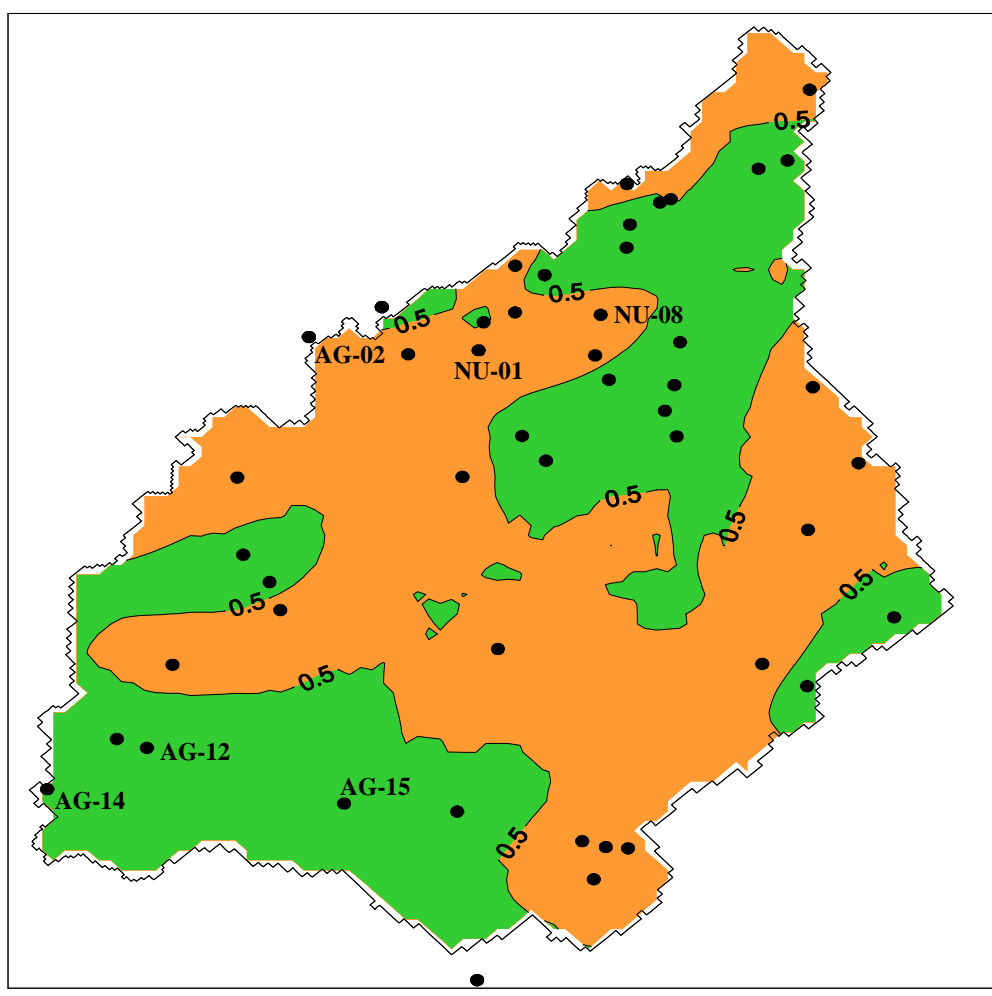
Figure 8. Recharge probability map from the study of Baehr and others (2002). The green area indicates <50% probability of exceeding a seasonal recharge rate of 29.2 cm/y, orange indicates >50% probability of exceeding a seasonal recharge rate of 29.2 cm/y, and black dots are sampling holes. Focus sites for this study are also indicated by well numbers.

METHODS

Unsaturated hydraulic properties were measured for each site and interpolated in several ways. The Darcian unit-gradient approach was used for estimating recharge under inferred, steady-flow conditions. Hydraulic properties were measured by the SSC method and also estimated from more easily measured bulk properties as a comparison. Four of the six sites were interpreted as having steady flow at least seasonally based on available water-content data (Baehr, 2002, personal communication). Numerical simulations were run in order to further assess steady flow conditions at site AG-02. For cases of unsteady flow, water-level data were used to estimate recharge based on the premise that rising water levels are caused by water entering the aquifer. Figure 9 illustrates in the form of a flow chart the various paths taken from measured data to recharge estimates. Table 2 shows the various methods used in this study including data required for each, principle of each method, possible variations, and number of possible combinations based on those variations. Methods are described in detail individually below.

Laboratory Measurements

Bulk Properties

Data required for this study include particle and bulk density and particle-size distributions. Particle-density measurements were performed with the pycnometer method (Flint and Flint, 2002a) on all core samples. Porosity was calculated using the
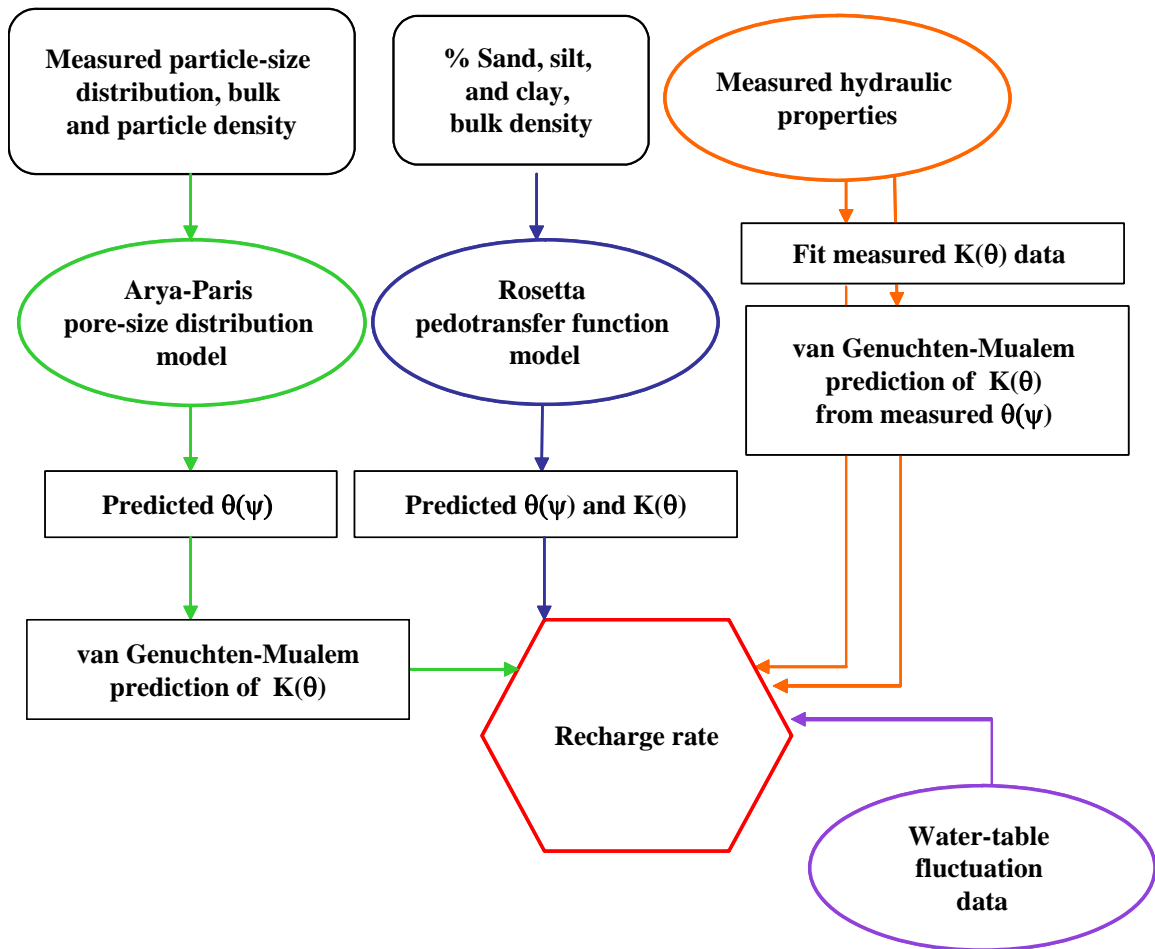
Figure 9. Methods flow chart illustrating the paths taken from measured data to recharge estimates.

Table 2. Methods used in this study including data required for each, principle of the methods, variations, and number of possible combinations based on those variations [K: hydraulic conductivity, K_{sat}: saturated hydraulic conductivity, θ: water content, θ_{sat}: saturated water content, θ_r: residual water content, ψ: matric potential, N/A: not applicable].

Method	Data required for method	Principle	Variations	Number of combinations
Measure and fit $K(\theta)$(Conca and Wright, 1998; Nimmo and others, 2002)	Measured $K(\theta)$	Measured points are interpolated to get $K(\theta)$ curve	Hand-drawn fit	1
			Power law fit	1
			Van Genuchten fit with θ_{sat} and θ_r fixed or optimized	2
Van Geuchten-Mualem (van Genuchten , 1989) predition of $K(\theta)$	Measured $\theta(\psi)$	Measured $\theta(\psi)$data are used to predict $K(\theta)$ curve	K_{sat}, θ_{sat}, θ_r fixed or optimized	3
Rosetta model (U.S. Department of Agriculture, 2001)	USDA textural information and bulk density	Neural network analysis of hydraulic property database to predict $K(\theta)$ curve from given input	Texture	1
			% sand, silt, clay	1
			% sand, silt, clay, bulk density	1
Arya-Paris model (Arya and Paris, 1981)	Particle size distribution and bulk density	Pore-size distribution is calculated and translated to $\theta(\psi)$ then to $K(\theta)$	K_{sat}, θ_{sat}, θ_r fixed or optimized	3
Total number of recharge estimates				**13**

relation $\Phi= 1-(\rho_{bulk}/\rho_{particle})$ using measured bulk- and particle- density values (Flint and

Flint, 2002b). A Coulter LS-230 particle-size analyzer was used to characterize particle-

size distributions for 21 samples by optical diffraction (Gee and Or, 2002). The range of

measurement for this device is from 4×10^{-5} to 2 mm, divided into 116 size bins. Any

particles above 2 mm were sieved out with ASTM sieves (sizes 2, 2.8, 4, 5.6, 8, 11.2, 16,

22.4, and 32.5 mm) and later integrated into the size-distribution results. The fraction

finer than 2 mm was carefully disaggregated using a mortar and rubber-tipped pestle,

and then split with a 16-compartment spinning riffler to obtain appropriate

representative samples for analysis. Each sample was then put into the fluid module of

the Coulter LS-230, which circulates the sample through the device, sonicated for 60

seconds prior to each run, and run twice in order to calculate an average for each sample.

Hydraulic Properties

The steady state centrifuge (SSC) method used to measure unsaturated hydraulic

conductivity (K) on 6 samples from within the study area is the Unsaturated Flow

Apparatus (UFA) version (Fig. 10) (Conca and Wright, 1998; Nimmo and others, 2002)

of the method originally developed by Nimmo and others (1987). Core samples were

collected throughout the unsaturated zone using a split-spoon sampler that was 61 cm

long and 5.1 cm in diameter. Field water contents at that time were also determined

gravimetrically. Each sample was recored in the laboratory using a mechanical recoring

device. Liners were secured by clamps as the material was slowly extruded upward into

a 4.9-cm-long, 3.3-cm-diameter retainer with a sharp-edged coring attachment that was

custom made from stainless steel. The retainers are designed specifically to fit into the

buckets of the UFA centrifugal rotor.

The SSC method, used for the determination of K as a function of water content

(θ), requires that steady-state conditions be established within a sample under centrifugal

force. Steady-state conditions require a constant flow rate and a constant centrifugal

force for sufficient time that both the water conditions and the water flux within the

sample are constant. When these conditions are satisfied, Darcy's law relates K to θ and
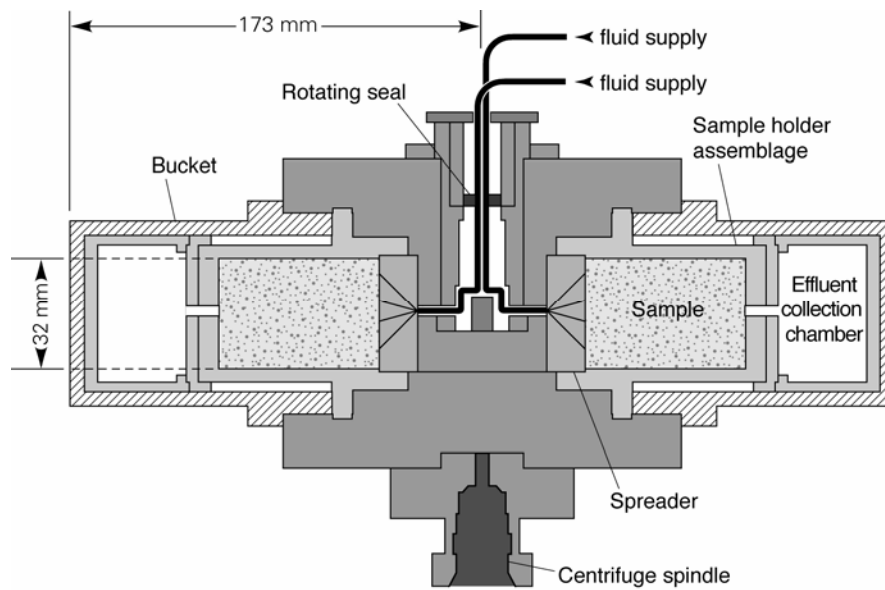
Figure 10. Cross section of the Unsaturated Flow Apparatus (UFA) rotor used in unsaturated hydraulic conductivity measurements. The rotor holds 2 samples and 2 counterweights (not shown) for balance.

matric pressure (ψ) for the established conditions.

With centrifugal instead of gravitational force, Darcy's law takes the form

$$q = -K(\theta)\left(\frac{d\psi}{dr} - C\rho\omega^2 r\right)$$

where: q = flow rate (LT^{-1})

C = unit conversion factor of 1 cm-water/980.7 dyne/cm^2 (1 cm of water

is equal to a pressure of 980.7 dyne/cm^2 and 1 dyne = 1 g cm/s^2)

ρ = density of the applied fluid (ML^{-3})

ω = angular velocity (T^{-1})

r = radius of centrifugal rotation (L)

If the driving force is applied with the centrifuge rotation speed large enough to ensure

that $d\psi/dr \ll \rho\omega^2 r$, i.e., any matric-pressure gradients that develop in the sample

during centrifugation are insignificant, the flow is essentially driven by centrifugal force

alone. The flow equation then simplifies to

$$q \approx K(\theta)C\rho\omega^2 r.$$

The ω threshold for which the $d\psi/dr$ gradient can become negligible depends on the soil

hydraulic properties. Nimmo and others (1987) discussed this gradient and presented

model calculations showing that it becomes negligible at relatively low speeds for a

sandy medium and at higher speeds for a fine-textured medium. This technique

normally results in a fairly uniform water content throughout the sample, permitting the

association of the sample average θ and ψ values with the measured K. After achieving

steady flow at a given q, a measurement of θ (by weight) and ψ (by non-intrusive

tensiometer (Young and Sisson, 2002)), and computation of K, yielded a triplet of data

(K, θ, ψ) for the average water content within the sample. Repeat measurements with

different q and in some cases different rotational speed gave additional points needed to

define the K(ψ), K(θ), and θ(ψ) characteristics. Table 3 shows the pump, centrifuge

settings, and run times used in the determination of the K(θ) relationship, though run

times commonly vary from sample to sample and often exceed those given as guidelines

for the method (Conca and Wright, 1998; Nimmo and others, 2002).

Table 3. Centrifuge run parameters and resulting hydraulic conductivity values measured in this study. Minimum run times are guidelines; actual times to reach steady state flow vary and often exceed these values.

Flow Rate (ml/hr)	RPM	Hydraulic Conductivity (cm/s)	Minimum Run Time (hours)
50	600	4.63E-05	1-2
50	1000	1.67E-05	1-2
50	1500	7.41E-06	1-2
40	2000	3.33E-06	2-3
15	2000	1.25E-06	2-3
5	2000	4.17E-07	5
1	2000	8.34E-08	8
0.5	2300	3.15E-08	10
0.1	2500	5.33E-09	10
0.01	2500	5.33E-10	10

Power Law and Hand Interpolation

Several curve fits were used to interpolate the measured unsaturated hydraulic

conductivity for use in recharge estimation. The curves were fit with 1) a simple power-

law function in the form of $y=mx^a$ where y and x are hydraulic conductivity and corresponding water content and m and a are fitted parameters, and 2) a hand interpolation following the laboratory-measured $K(\theta)$ points. Recharge rates from the power-law fits were determined using the fit-generated equations. Hand interpolation, though not a mathematically rigorous technique, was used to estimate recharge rates by visually picking values from the curve.

van Genuchten-Mualem Model

The measured water retention data were fit with the empirical formula of van Genuchten (1980) using the regression analysis program RETC (van Genuchten and others, 1991). The empirical formula has the form:

$$\theta(\psi) = \theta_r + \{(\theta_{sat} - \theta_r)/[1+(\alpha\psi)^n]^m\}$$

where: θ_r = residual water content (L^3/L^3)

θ_{sat} = saturated water content (L^3/L^3)

α, n, and m = empirical fitting parameters (dimensionless)

Using measured θ and ψ values, α and n parameters are optimized to achieve the best fit to the data. The parameter m is set equal to 1-1/n in order to reduce the number of independent parameters allowing for better model convergence and to permit convenient mathematical combination with Mualem's model (van Genuchten, 1980). The van Genuchten equation is used in conjunction with the pore-size-distribution model of Mualem (1976) to yield the van Genuchten-Mualem (vGM) model (van Genuchten, 1980) for K:

$$K = K_{sat} S_e^{\ L} \left\{ 1 - [1 - S_e^{\ n/(n-1)}]^m \right\}^2$$

where: K_{sat} = saturated hydraulic conductivity (L/T)

L = curve-fitting parameter (dimensionless)

$$S_e = \frac{\theta - \theta_r}{\theta_{sat} - \theta_r} \quad \text{(dimensionless)}$$

Alternative empirical representations for matric potential and hydraulic conductivity exist; however, the models given by the equations above are most commonly used. The vGM model is used directly as a curve-fitting technique or in conjunction with other models as described in the following sections.

Arya-Paris and van Genuchten-Mualem Models

The Arya-Paris model (Arya and Paris, 1981) is a method of estimating water retention from more easily measured textural data. This model uses particle-size distribution data, bulk density, and particle density along with capillary theory to predict the $\theta(\psi)$ function for a given medium. This information may then be used, with one measured K value, in the vGM model equations described above to estimate hydraulic conductivity and ultimately recharge rates.

A pore-size distribution is calculated by the model from the particle-size distribution by associating discrete particle-size fractions with an estimated pore volume for that fraction using the equation:

$$V_{vi} = (W_i/\rho_p)e; \quad i = 1, .2, ..., n$$

where: V_{vi} = pore volume (L^3) per unit sample mass associated with particles in

the ith particle size range

W_i = solid mass (M) associated with particles in the ith particle size range

taken from the particle size distribution

ρ_p = particle density (ML^{-3})

$e = (\rho_p - \rho_b) / \rho_b$ (dimensionless)

ρ_b = bulk density (ML^{-3})

Pore volumes that correspond to each size range are progressively accumulated and

considered filled with water to estimate water contents for various matric pressures to be

used in the retention curve. The water contents are paired with corresponding matric

pressure (ψ) values by the capillary equation (Jury and others, 1991):

$$\psi = \frac{2\gamma \cos \theta}{\rho_w g r}$$

where: γ = surface tension of water ($ML^{-1}T^{-2}$)

θ = contact angle (assumed to be zero)

ρ_w = density of water (ML^{-3})

g = gravitational acceleration (LT^{-2})

r = pore radius (L) corresponding to the incremental filled volume

The water-content and pressure values are paired to form the water-retention curve. The

water-retention curve is then used to estimate hydraulic conductivity using the vGM

model as described above.

<u>Rosetta Model</u>

Hydraulic properties can be estimated indirectly with the Rosetta model (U.S. Department of Agriculture, 2001) using more easily measured soil properties such as sediment texture and bulk density. The Rosetta model uses neural-network analysis to estimate values of the parameters α and n utilized in the vGM equations by comparison with a database of measured hydraulic and textural properties for a large number of diverse soils. In very basic terms, the program, by way of network analysis, searches out the best hydraulic-data match given the input data. The Rosetta program is described in detail by Schaap and Leij (1998), Schaap and others (1998), and Schaap and others (1999).

Neural networks can be used to discern patterns where data are incomplete or where there is a large number of input variables (Pachepsky and others, 1996). The neural network uses many interconnected computational nodes, each of which can use multiple input variables to give a single output. In essence, the neural network approximates functions, much like regression analysis, but has been shown to give better results where there are more than three variables (Pachepsky and others, 1996). In the Rosetta model, the neural-network approach allows for the best possible prediction of hydraulic properties from a large number of samples within the model's database. The model uses the UNSODA database (U.S. Department of Agriculture, 2001), which contains data for hundreds of soil samples, many agricultural, with properties measured by a wide variety of techniques.

For this application, measured bulk density and the fractions of sand, silt, and clay are used as input to obtain estimates for curve-fitting parameters θ_r, θ_s, n, α, K_{sat}, and L, which are used in the vGM functions. The model uses the input data in the neural-network analysis of the database of measured properties. The estimated hydraulic properties are then used to estimate recharge rates.

Darcian Recharge Estimation

Once the hydraulic conductivity has been measured, recharge may be estimated as described below using the unit-gradient assumption. If it is assumed that flow under field conditions is steady and driven by gravity alone, then, according to Darcy's Law, recharge will be numerically equal to the hydraulic conductivity of the material at the measured in-situ water content. The Darcian unit-gradient method (Sammis and others, 1980, Nimmo and others, 1994) is generally used to estimate long-term average recharge rates in arid regions with thick unsaturated zones where, below some depth, flow is considered to be steady and driven by gravity alone. In the coastal plain environment evaluated in this study , there appear to be locations where, below a certain depth, changes in water content are slight and recharge rates may then vary little over the course of the year or may exhibit a seasonal, repetitive pattern of variability.

In the unsaturated zone, Darcy's Law may be represented by the equation:

$$q = -K(\psi)\left(\frac{d\psi_{total}}{dz} - \frac{dz}{dz}\right)$$

where: q = flow rate (LT^{-1})

K = hydraulic conductivity (LT^{-1})

$\dfrac{d\psi_{total}}{dz}$ = matric potential gradient (dimensionless)

$\dfrac{dz}{dz}$ = gravitational potential gradient (dimensionless)

Under the unit-gradient assumption, matric and solute potential are constant with depth

(i.e., $\dfrac{d\psi_{total}}{dz} = 0$) and gravity is the only driving force (i.e., $\dfrac{dz}{dz} = 1$), therefore q is equal

to the hydraulic conductivity of the medium as a function of water content (θ). If the in-situ water content is known and unchanging in time, and the K corresponding to the in-situ water content is known as well, that K may be interpreted as a recharge rate. Because unsaturated hydraulic conductivity is seldom measured at the exact field water content, interpolation of the measured, highly non-linear K(θ) relationship is critical to recharge estimation.

Water Table Fluctuation Method

The water table fluctuation (WTF) method is based on the assumption that changes in groundwater levels can be attributed to recharge entering the aquifer. This process is represented by

$$R = S_y \frac{dh}{dt}$$

where: R = recharge (LT^{-1})
           S_y = specific yield (dimensionless)
           h= water table height (L)

t = time (T)

The method is generally used over short time intervals, though it can be used to estimate seasonal or annual changes in subsurface storage, which essentially represents net recharge over that period (Healy and Cook, 2002). Net recharge is the total change in subsurface storage for a given period without information on shorter intervals of recharge and discharge. The change in height of the water table is determined by taking the difference between the measured rising limb and the antecedent recession curve that would naturally result in the absence of recharge. An exponential decay function based on the water table elevation during the falling limb of the recession curve was used to predict antecedent water levels over a period of about 6 years from 1996 to 2002 for which data were available from the USGS (Fig. 11).

Specific yield is the ratio of the volume of water that will drain by gravity after saturation and the total volume of material. Specific yield is considered to be independent of time and assumes instantaneous drainage, which is not the case in reality. Soils can take a long time to drain depending on texture, although in this case, because the material is sandy, rapid drainage is considered a reasonable approximation. Published values from 17 studies indicate that specific yield ranges from 0.21 to 0.27 for sandy material (Johnson, 1967). In this study, a value of 0.27 for specific yield was directly determined from water-retention curves measured in the laboratory (described above) as a part of this study. This method of determining specific yield from water retention is suggested by dos Santos and Young (1969) and Duke (1972) for sandy material. Those authors found that specific yield was reasonably approximated as
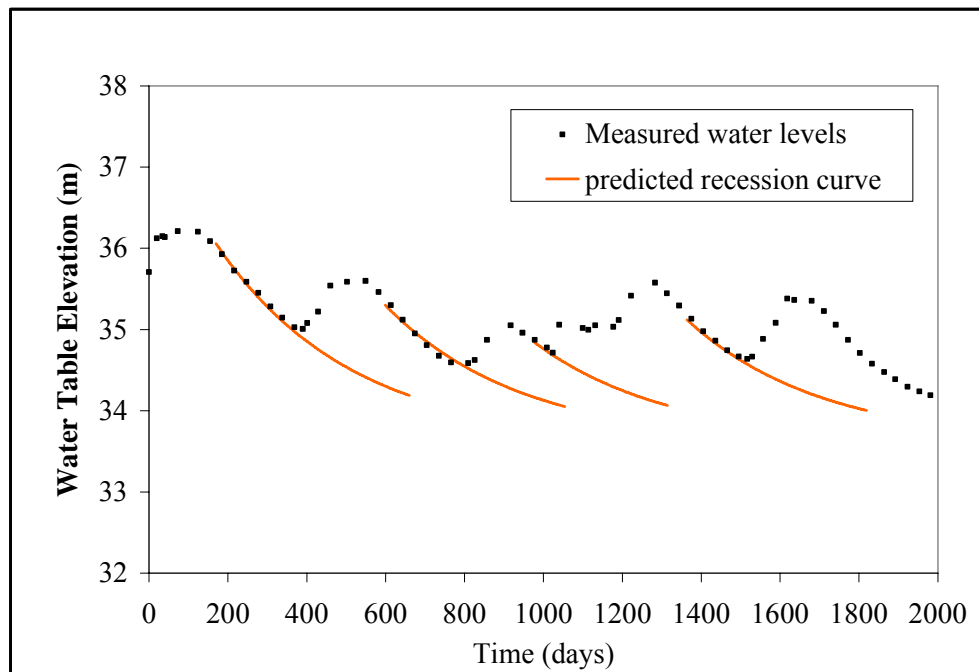
Figure 11. Well AG-02 water levels (U.S. Geological Survey, 2003) and predicted recession curves based on an exponential decay function applied to the measured falling limb data. Data are from the period of October 7, 1996 (day 0) through May 28, 2002 (day 2000).

$$S_y = \phi - \theta(H)$$

where: ϕ = porosity (dimensionless)

              θ = volumetric water content (dimensionless)

              H = depth to the water table (L)

The $\theta(H)$ value is determined by assuming that the known depth to water table (H)

corresponds to that same value of ψ on the measured $\theta(\psi)$ curve. The corresponding θ

may then be calculated using the van Genuchten equation (van Genuchten, 1980) with

the known fitted parameters. The effect of the depth to the water table on specific yield

was evaluated by Duke (1972). For fine sand it was found that specific yield is basically

constant with a depth to water of ~150 cm or greater. The depth-to-water dependence of

specific yield is generally greater for finer materials.

The WTF method was used to estimate recharge for the northern sites where

available data from 3 wells were spatially and temporally dense enough to be evaluated

reasonably. Patterns and magnitude of rise and fall are also almost identical for the 3

wells (Fig. 12); therefore the well with the densest data set, AG-02, was used in

estimating recharge. Details for the 3 wells are shown in Table 4.

Numerical Modeling: VS2DT

Utilizing laboratory-measured, parameterized unsaturated-hydraulic properties

($K(\theta)$ and $\theta(\psi)$ from the SSC method) as well as estimated parameters from the Rosetta

model for a layer for which only the particle-size distribution is known, seasonal

infiltration was simulated in one dimension using the U.S. Geological Survey variable-
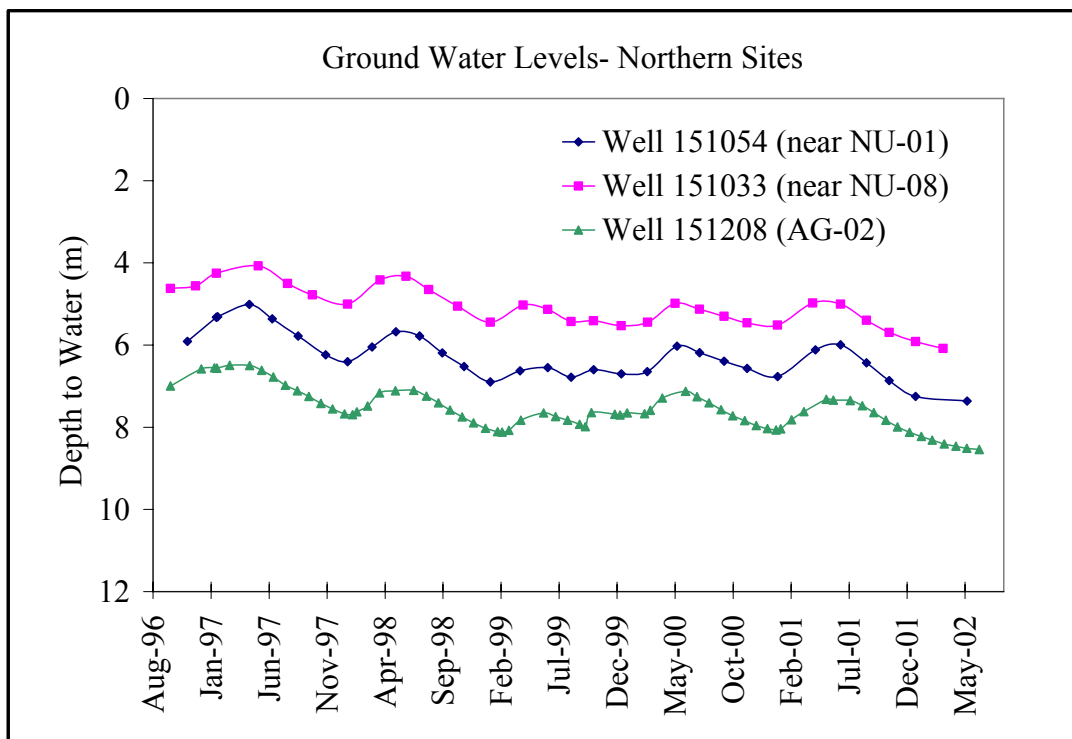
Figure 12. Ground water levels for three wells (U.S. Geological Survey, 2003) at or near the northern focus sites that were evaluated for the water table fluctuation method.

Table 4. Wells used in water table fluctuation estimates of recharge for the northern area of the study site.

Well (Alias)	Location	Well Depth/Comments
USGS 394354075025901 (aka WTMUA Monitoring 1OBS)	Lat. 39°43'54.0" Long. 75°02'59.0" (NAD 27)	16.46 m Closest monitored well to NU-08
USGS 394221075072201 (aka USGS GSC-1 Shallow OBS)	Lat. 39°42'21.0" Long. 75°07'22.0" (NAD 83)	10.97 m Closest monitored well to NU-01
USGS 394256075101001 (aka USGS AG-02, LINJ AG-02)	Lat. 39°43'02.6" Long. 75°10'12.4" (NAD 83)	10.06 m This well is AG-02

saturation model VS2DT (Lappala and others, 1983; Healy, 1990; Hsieh and others, 1999) in order to assess the steadiness of flow at site AG-02. VS2DT solves the finite difference approximation to Richards' equation (Richards, 1931) for flow and the advection-dispersion equation for transport. The flow equation is written with total hydraulic potential as the dependent variable to allow straightforward treatment of both saturated and unsaturated conditions. Cartesian or radial coordinate systems may be used. Several boundary conditions specific to unsaturated flow may be utilized including ponded infiltration, evaporation, plant transpiration, and seepage faces.

As input, the model requires saturated hydraulic conductivity, porosity, parameterized unsaturated hydraulic conductivity and water retention functions, grid delineation, and initial hydraulic conditions. Relations between pressure head, water content, and relative hydraulic conductivity may be represented by functions developed by van Genuchten (1980), Brooks and Corey (1964), Haverkamp and others (1977), or

by tabular data. The van Genuchten function was used in this study. Measured

hydraulic properties at two depths were used to determine the necessary input

parameters using the RETC code of van Genuchten and others (1991). Initial hydraulic

conditions may be specified as static equilibrium, pressure head, or water content.

Because data were available, water content was used as the initial condition. Boundary

conditions may include pressure or total head, flux, infiltration with ponding,

evaporation, plant transpiration, and seepage faces. In this study, a flux boundary was

used at the land surface to simulate precipitation.

The model domain was established to be 3.5 m wide and 8.5 m deep. The

hydraulic properties within the model domain were assigned based on layer designations

determined from core and bulk samples and lithologic logs (Table 1), measured

hydraulic properties from two depths and particle-size distributions. A three-layer

system was chosen with layers from 0 to 1.2 m, 1.2 to 5.5 m and 5.5 to 8.5 m (Fig.13).

The simulation period chosen to evaluate the observed steady flow condition for site

AG-02 is October 6, 2000 to March 12, 2001. This period was chosen because 1) field

water contents were measured on the first and last day of the simulation period, 2) the

simulation period includes mainly the time of year when ET is negligible and can

therefore be ignored, 3) precipitation data were available for the entire period, and 4) the

period was sufficiently short that precipitation data could be prescribed on a daily basis.

The initial condition used in this study is the measured in-situ water content determined

at the beginning of the simulation period (Fig. 5). Boundary conditions are specified in

terms of flux out (water is allowed to leave the model domain) at the bottom boundary

← 3.5 m →

8.5 m

Layer 1: 0-1.2 m, Coarse sand and gravel, Rosetta-predicted hydraulic properties

Layer 2: 1.2-5.5 m, Fine sand with some small gravel, measured hydraulic properties

Layer 3: 5.5-8.5 m, Coarse sand with little gravel, measured hydraulic properties

7.75 m Water Table
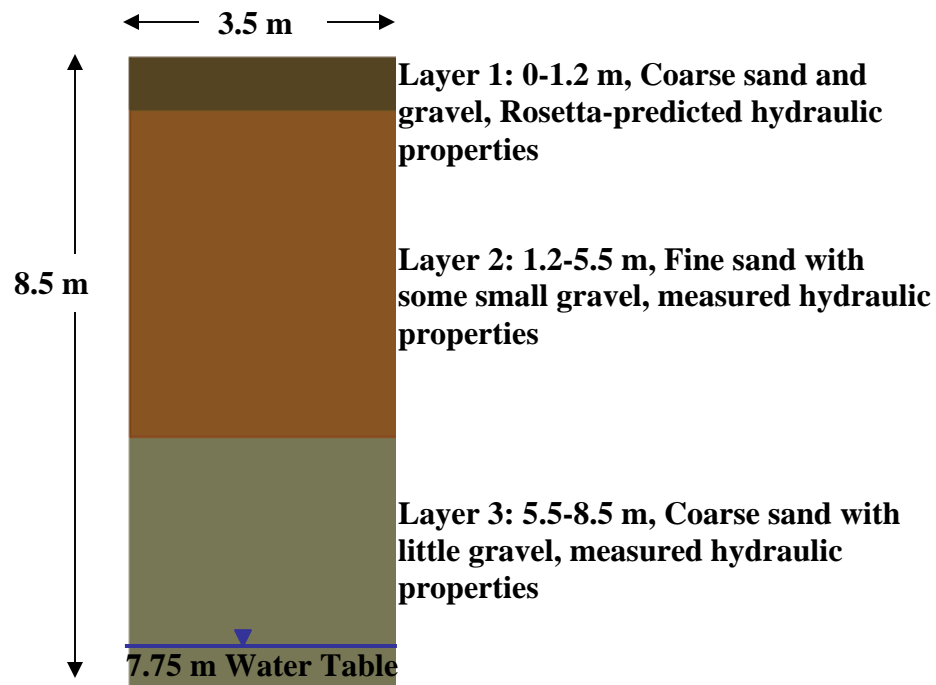
Figure 13. VS2DT model domain for site AG-02 with designated layering based on hydraulic and bulk property data. Rosetta-estimated hydraulic properties were used for layer 1 from 0 to 1.2 m and measured hydraulic properties were used for layer 2 from 1.2 to 5.5 m and layer 3 from 5.5 to 8.5 m. Because there were no data below 6.1 m, material was assumed to be the same as that above so that the model could include material below the water table.

and side boundaries below the water table, no-flow at the lateral boundaries above the

water table, and flux in equal to natural precipitation at the land surface based on

climatic data (Fig. 14). The flux-out boundary condition below the water table was

chosen in order to simulate natural ground water flow away from the model domain. If

water were not allowed to leave the domain, as it would naturally due to ground water

flow, the water table would rise unrealistically. Because there are no data available to

assess head gradients, a flux value of 0.00086 m/d was chosen to match as closely as

possible the measured water table elevation. Precipitation records from the National

Oceanic and Atmospheric Administration's Glassboro 2 weather station (ID 283291) for

the modeled period are shown in Figure 14. The period of simulation was considered to

have negligible ET, therefore all of the recorded precipitation was considered as flux

into the subsurface.
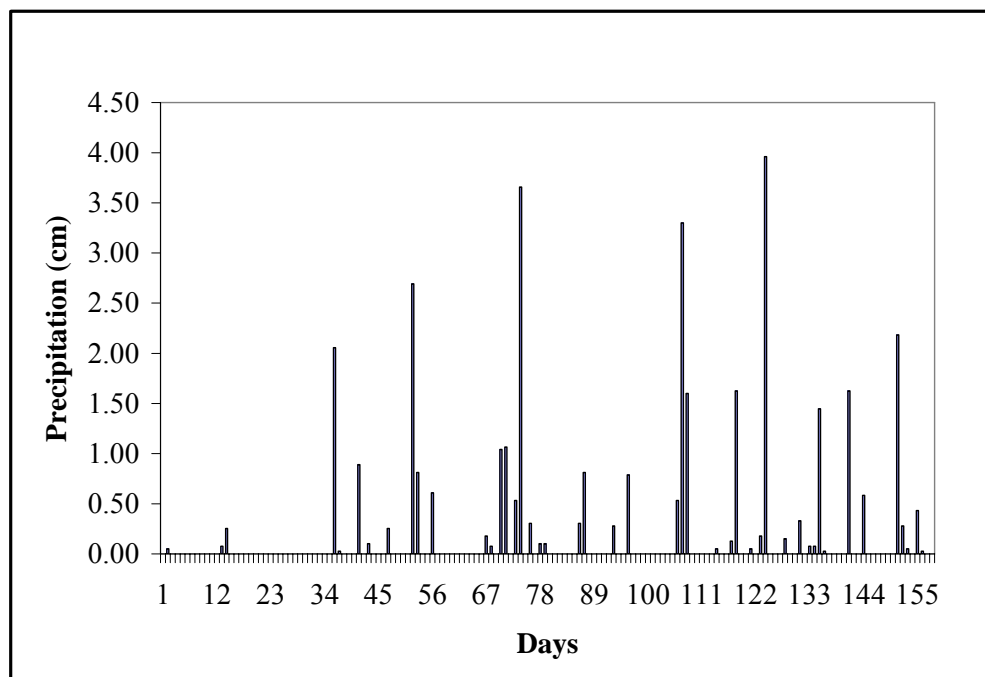
Figure 14. Daily precipitation data used in modeling from the National Oceanic and Atmospheric Administration's Glassboro 2 weather station (ID 283291). Days are numbered starting on October 6, 2000.

RESULTS

At the beginning of this study, each site was characterized as having an inferred flow regime (Fig. 15) interpreted solely from the measured profiles of field water content. This characterization provided a starting point for the evaluation of recharge at each site individually and for comparison among sites on that basis. The hypothesized regimes were steady flow, seasonally steady flow, and unsteady flow. Initially, sites AG-02 and AG-14 were characterized as having steady flow year round, sites AG-12 and NU-08 as having seasonally steady flow, and sites AG-15 and NU-01 as having unsteady flow (Fig. 15). For brevity, the term "recharge" is used to indicate a vertical flow rate at a point in the unsaturated zone, even though in some cases it is not fully established that the data represent a true recharge rate.

Laboratory Measurements

Bulk Properties

Particle-size distributions were measured for 21 samples (Table 5; Figs. 16 - 18). Results show that the materials are generally coarse, gravelly sand to sandy loam according to the U.S. Department of Agriculture textural classification scheme (Soil Survey Staff, 1975) used in this study. Clay content ranges from 0.4 to 4.5 %, silt from 1.6 to 38.1 %, sand from 53.9 to 97.8 %, and gravel from 0 to 27.5 % (Table 5). Bulk density, particle density, calculated porosity, and field water contents determined at the time of core collection are summarized in Table 6. Field water contents shown here
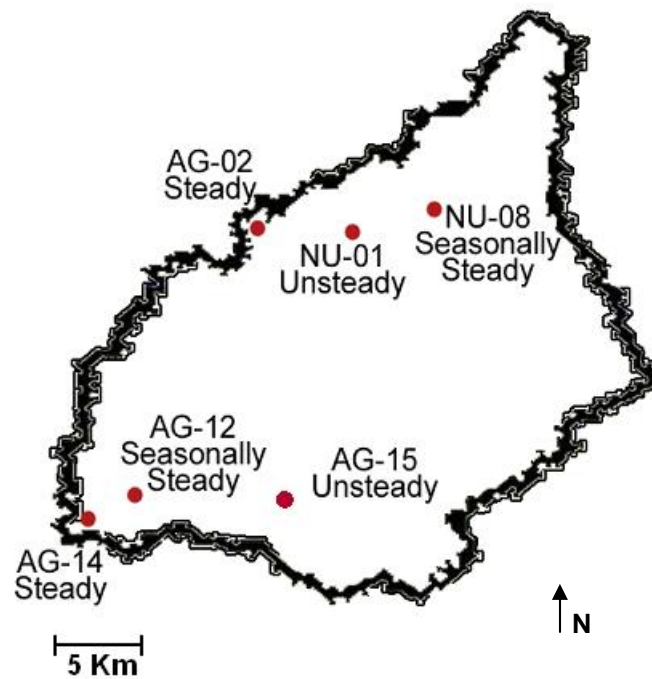
Figure 15. Outline of study area with focus sites and hypothesized flow regimes based on examination of measured field water contents. Sites were designated as having steady, seasonally steady, or unsteady flow as a starting point for individual and comparative evaluation.

Table 5. USDA (Soil Survey Staff, 1975) texture and textural class percentages for core and bulk samples.

Site	Depth (m)	% Clay (<2μm)	% Silt (2-50 μm)	% Sand (50-2000 μm)	% Gravel (>2000 μm)	USDA Texture
AG-02	1.2	2.4	11.8	72.6	13.2	Sand
	2.1	2.2	11.2	75.2	11.4	Sand
	4.3	1.0	5.4	88.4	5.2	Sand
	6.1	0.9	4.1	85.7	9.3	Sand
AG-14	1.8	2.6	16.1	53.9	27.5	Gravelly Loamy Sand
	3.7	4.5	38.1	57.4	0.0	Sandy Loam
	5.5	0.9	2.7	96.4	0.0	Sand
AG-12	1.2	2.2	22.1	60.8	14.9	Loamy Sand
	2.4	0.4	1.8	97.8	0.0	Sand
	3.7	0.7	2.4	95.2	1.7	Sand
	4.9	1.9	7.1	91.0	0.0	Sand
NU-08	1.8	1.5	9.8	74.7	14.0	Sand
	3.7	0.7	4.4	75.8	19.1	Gravelly Sand
	5.5	1.1	6.6	92.3	0.0	Sand
AG-15	1.8	1.0	3.5	92.6	2.9	Sand
	2.4	2.0	10.2	69.0	18.8	Gravelly Sand
	3.0	2.2	11.5	76.6	9.7	Sand
	4.9	1.5	7.4	91.1	0.0	Sand
NU-01	1.8	2.6	17.2	70.9	9.3	Loamy Sand
	5.5	3.5	27.6	67.2	1.7	Sandy Loam
	6.7	3.5	22.0	73.5	1.0	Sandy Loam
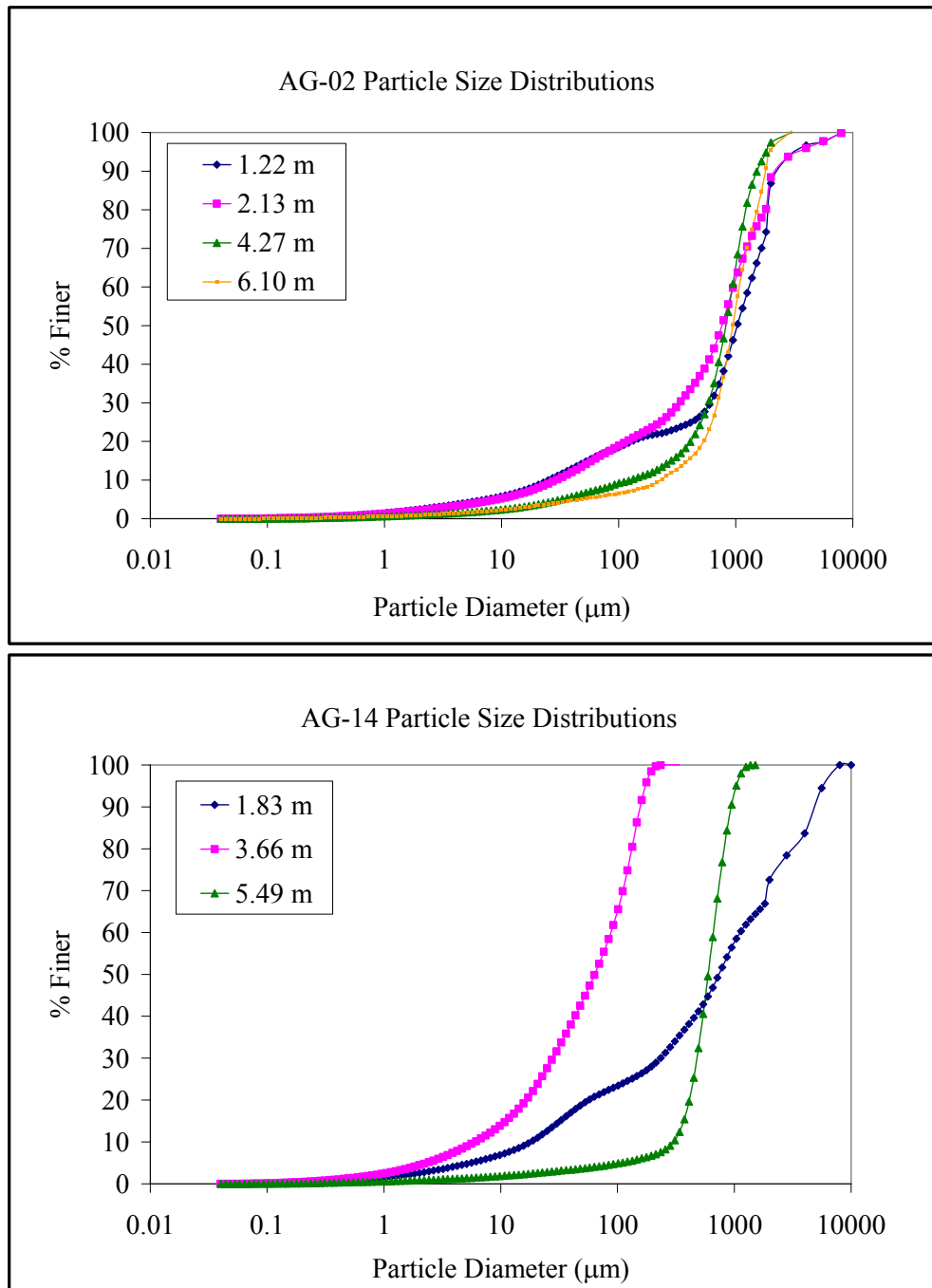
Figure 16. Cumulative particle-size distributions at various depths for steady flow sites AG-02 and AG-14.
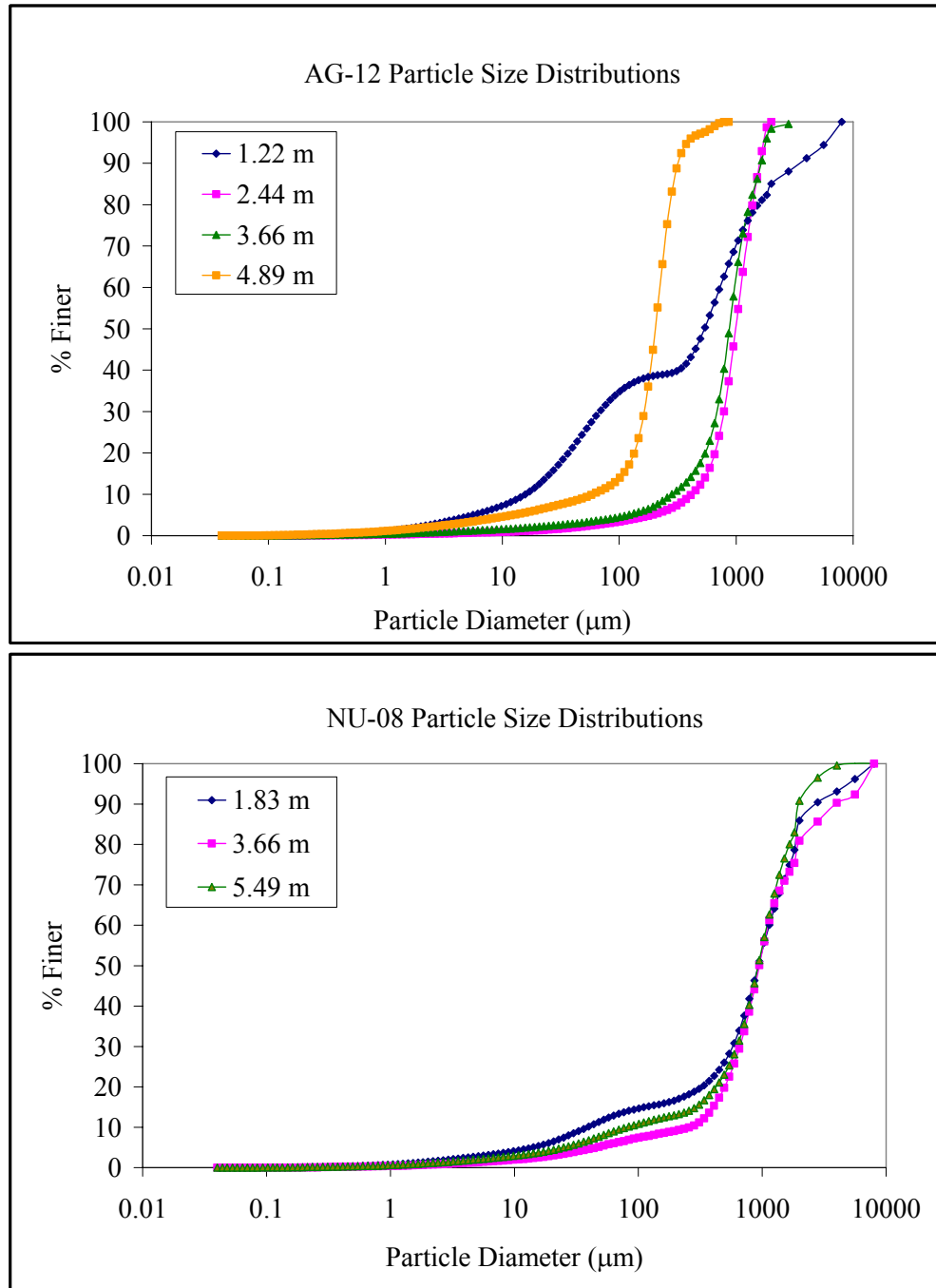
Figure 17. Cumulative particle-size distributions at various depths for seasonally steady flow sites AG-12 and NU-08.
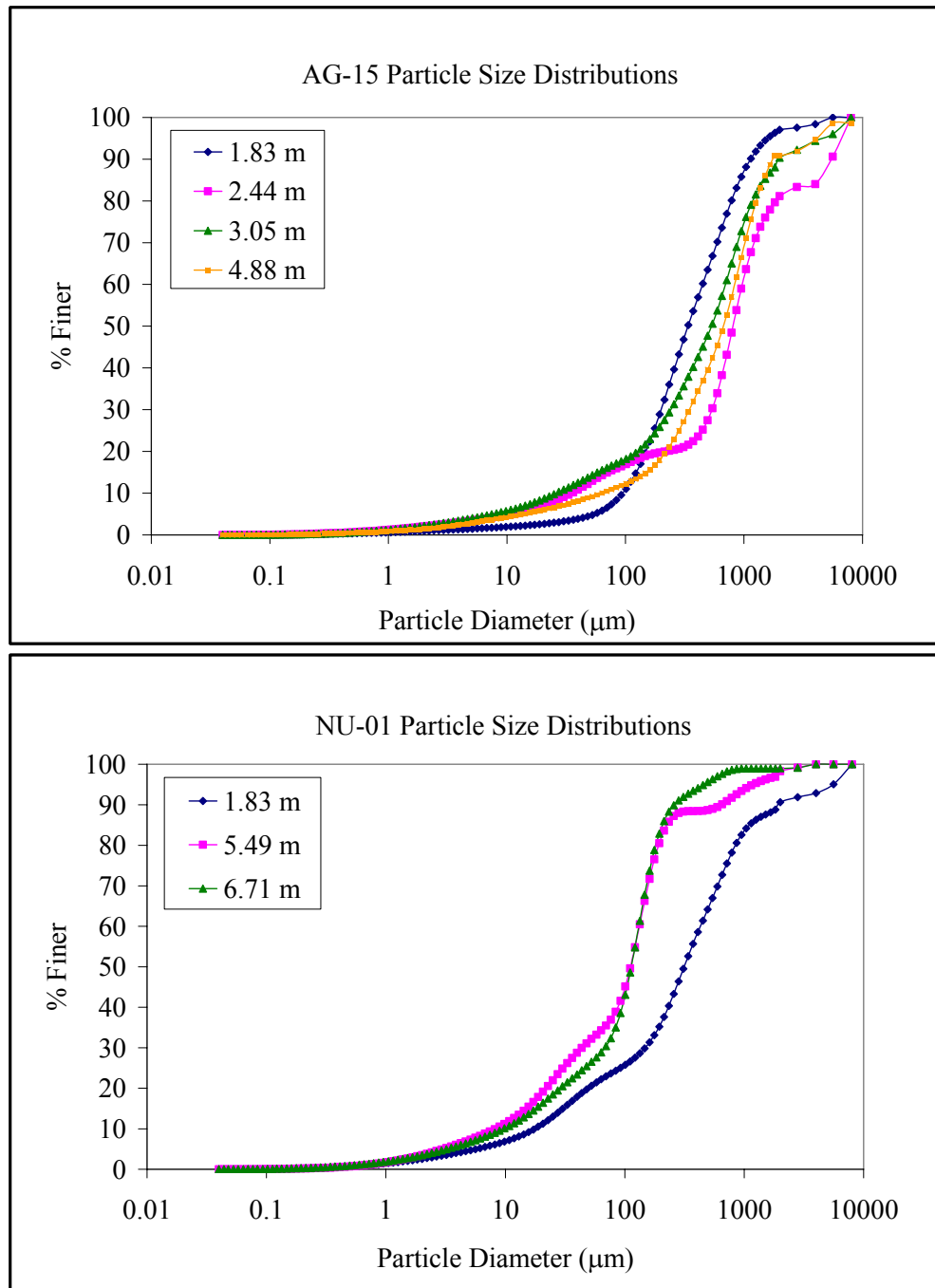
Figure 18. Cumulative particle-size distributions at various depths for unsteady flow sites AG-15 and NU-01.

Table 6. Bulk properties of core samples including field water contents determined at the time of collection.

Sample and Depth	Bulk Density (g/cm^3)	Particle Density (g/cm^3)	Calculated Porosity	Field Water Content (vol/vol)
AG-02 6.1 m	1.69	2.70	0.375	0.093
AG-14 5.5 m	1.63	2.81	0.421	0.049
AG-12 4.9 m	1.49	2.75	0.460	0.074
NU-08 5.5 m	1.77	2.75	0.357	0.117
AG-15 4.9 m	1.75	2.75	0.365	0.087
NU-01 6.7 m	1.64	2.75	0.404	0.131

were measured on cores collected at the same time as and adjacent to the cores used in the hydraulic property measurements. Bulk-density values range from 1.49 to 1.77 g/cm^3. Particle-density values range from 2.70 to 2.81 g/cm^3. Porosity was calculated using the relation $\Phi = 1 - (\rho_{bulk}/\rho_{particle})$ using measured bulk- and particle- density values (Flint and Flint, 2002b).

Hydraulic Properties

Unsaturated hydraulic conductivity (Fig. 19) was measured by the SSC method as described above on minimally disturbed core samples from each site (Figs. 5 - 7). Two samples were analyzed for site AG-02 from depths of 4.3 m and 6.1 m. The measured properties of both samples were used in numerical simulations (4.3-m sample is not shown in Fig. 19). The unsaturated hydraulic conductivity curve for the deeper
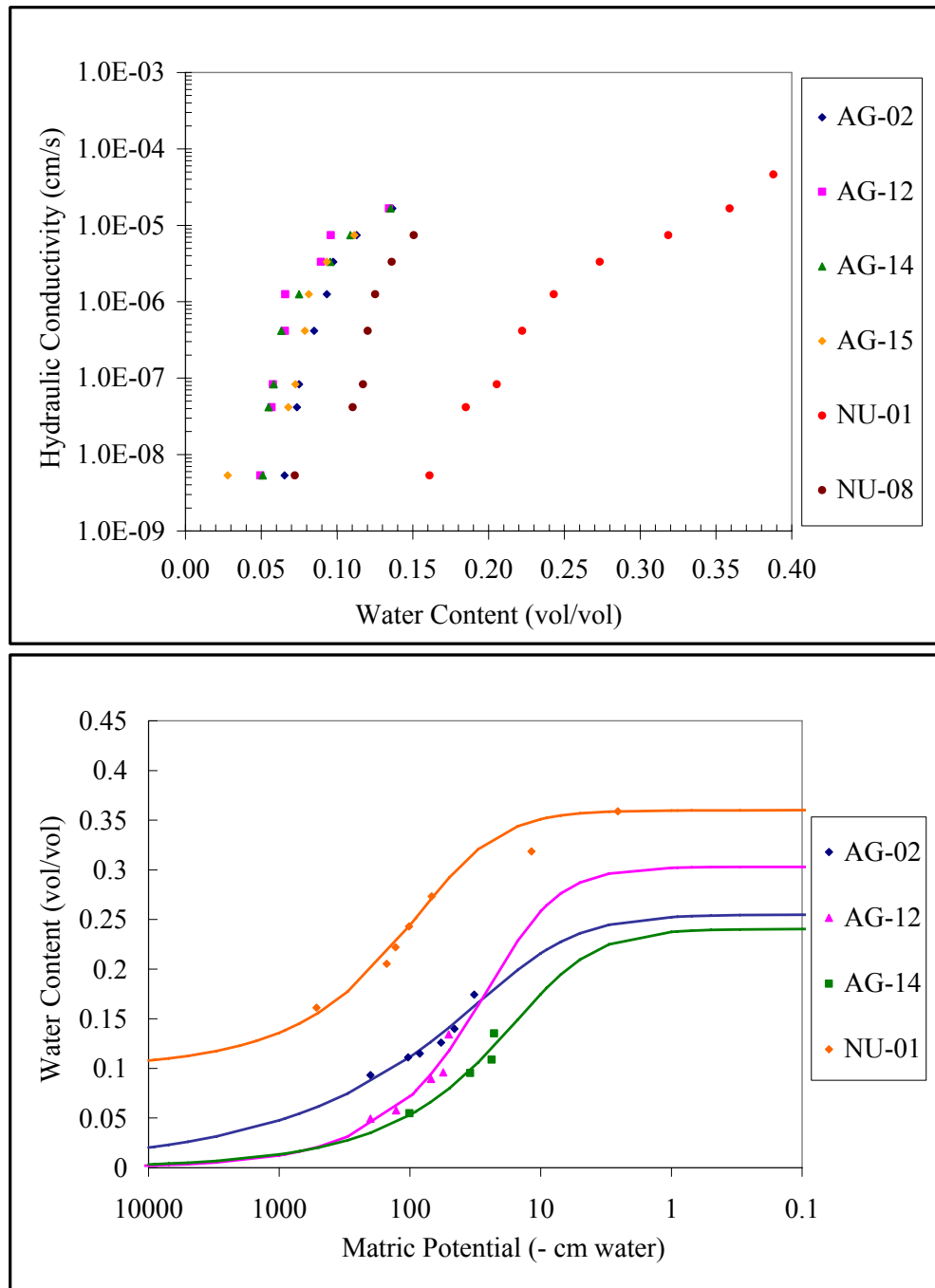
Figure 19. Laboratory-measured data points of hydraulic conductivity as a function of water content in upper panel. Water retention, in lower panel, is defined as water content as a function of matric potential. Water retention data points are fit with the empirical van Genuchten function (van Genuchten, 1980). Data are shown for each well, though water retention was not measured for wells AG-15 and NU-08.

sample (Fig. 19) was used in the recharge estimation because it was from the depth

below which flow was inferred to be steady. Water retention was measured as described

above on all cores (Fig. 19) except those from AG-15 (characterized as having unsteady

flow) and NU-08 (characterized as having seasonally steady flow) due to high gravel

contents, which prohibited adequate contact between the media and the tensiometer.

Results show the extreme sensitivity of hydraulic conductivity to very small changes in

water content, though the sensitivity is less pronounced in the case of NU-01

(characterized as having unsteady flow), which has the highest clay content of all of the

core samples.

Hydraulic Conductivity: Curve Fits and Predictions

Power Law and Hand Interpolation

Measured hydraulic-conductivity data (Fig. 19) were fit with a simple power-law

function and hand interpolated (Figs. 20-22) as described above. This provided an

additional means to estimate recharge rates for comparison (see discussion below) to the

more commonly used van Genuchten-Mualem curve fits.

van Genuchten-Mualem Fits and Predictions

Measured hydraulic-conductivity data were fit and also predicted with the vGM

model using the RETC program as described above. Figures 23 and 24 show results of

various fits for steady flow sites AG-02 and AG-14, seasonally steady flow site AG-12,

and unsteady flow site NU-01. This approach was not taken for seasonally steady flow
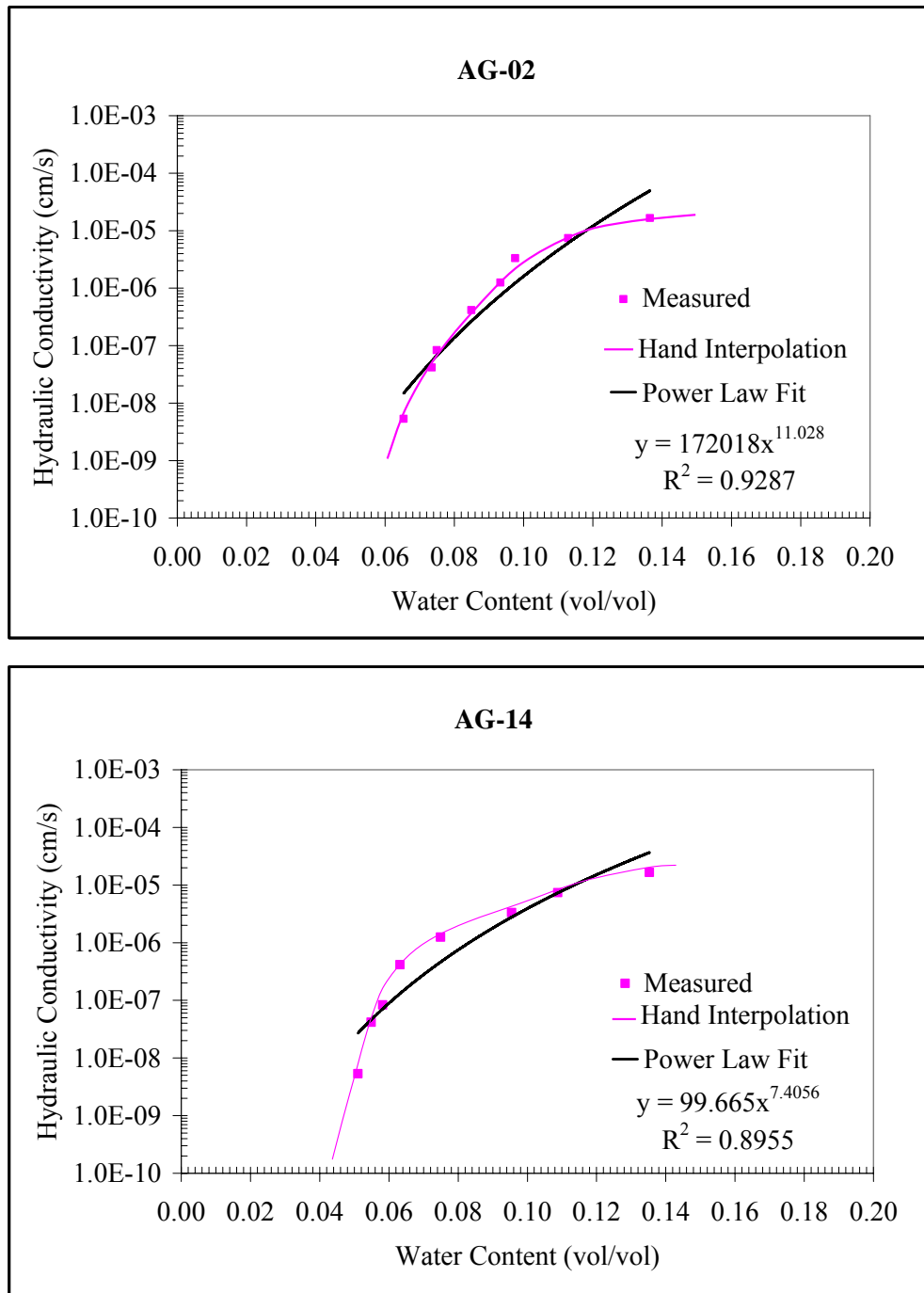
Figure 20. Hand interpolation and power-law fits to measured hydraulic conductivity data points for steady flow sites AG-02 and AG-14.
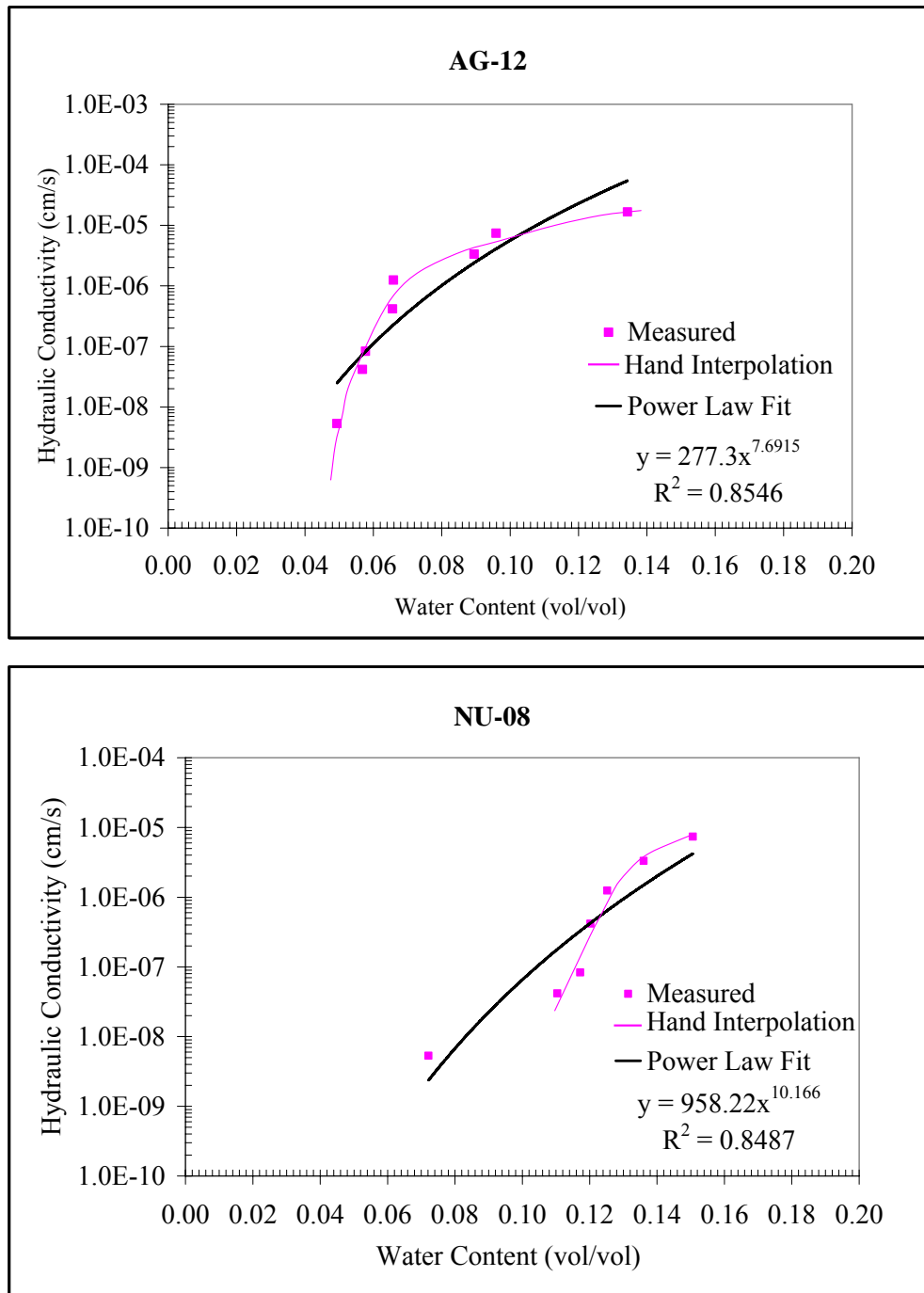
Figure 21. Hand interpolation and power-law fits to measured hydraulic conductivity data points for seasonally steady flow sites AG-12 and NU-08.
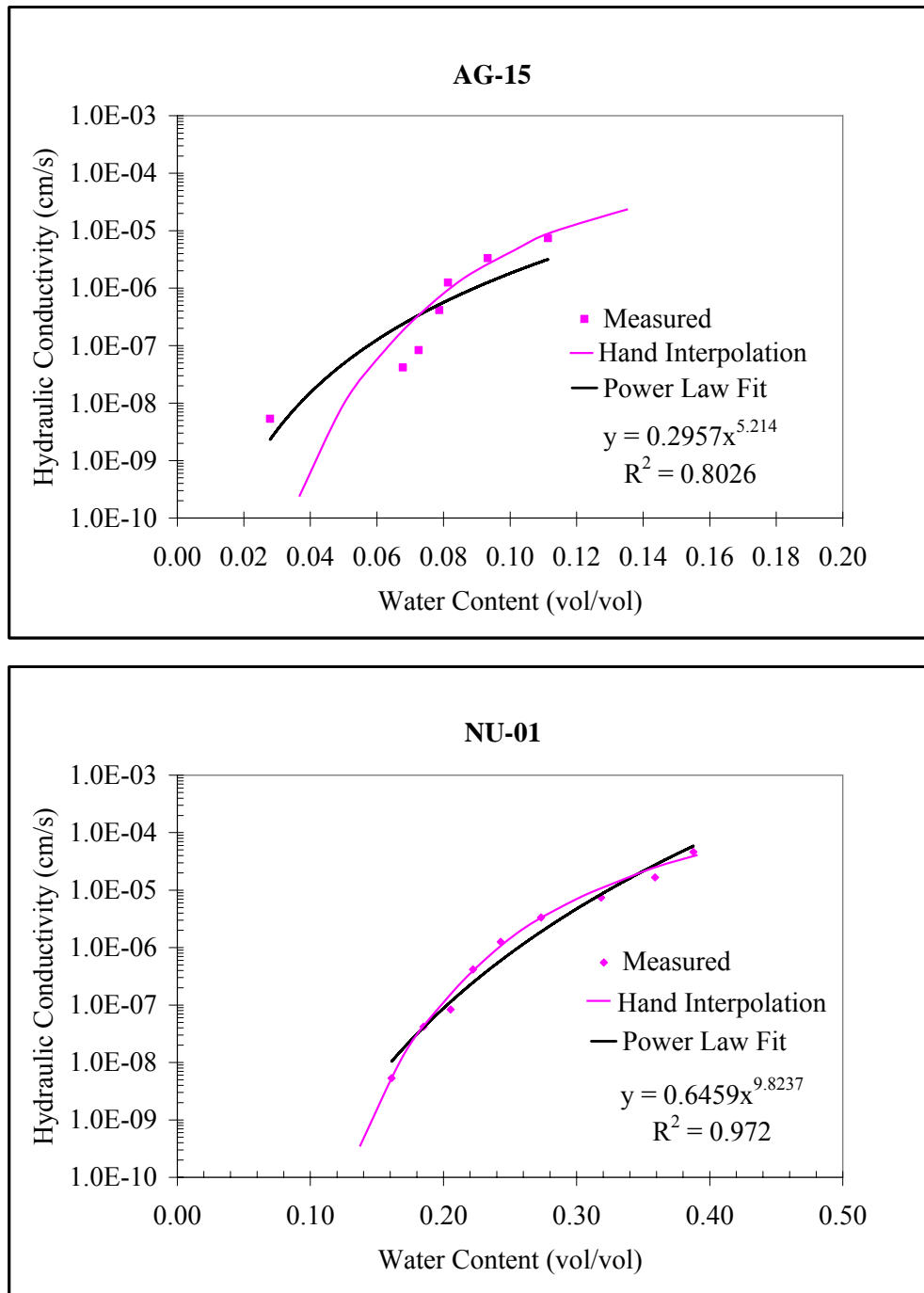
Figure 22. Hand interpolation and power-law fits to measured hydraulic conductivity data points for unsteady flow sites AG-15 and NU-01.
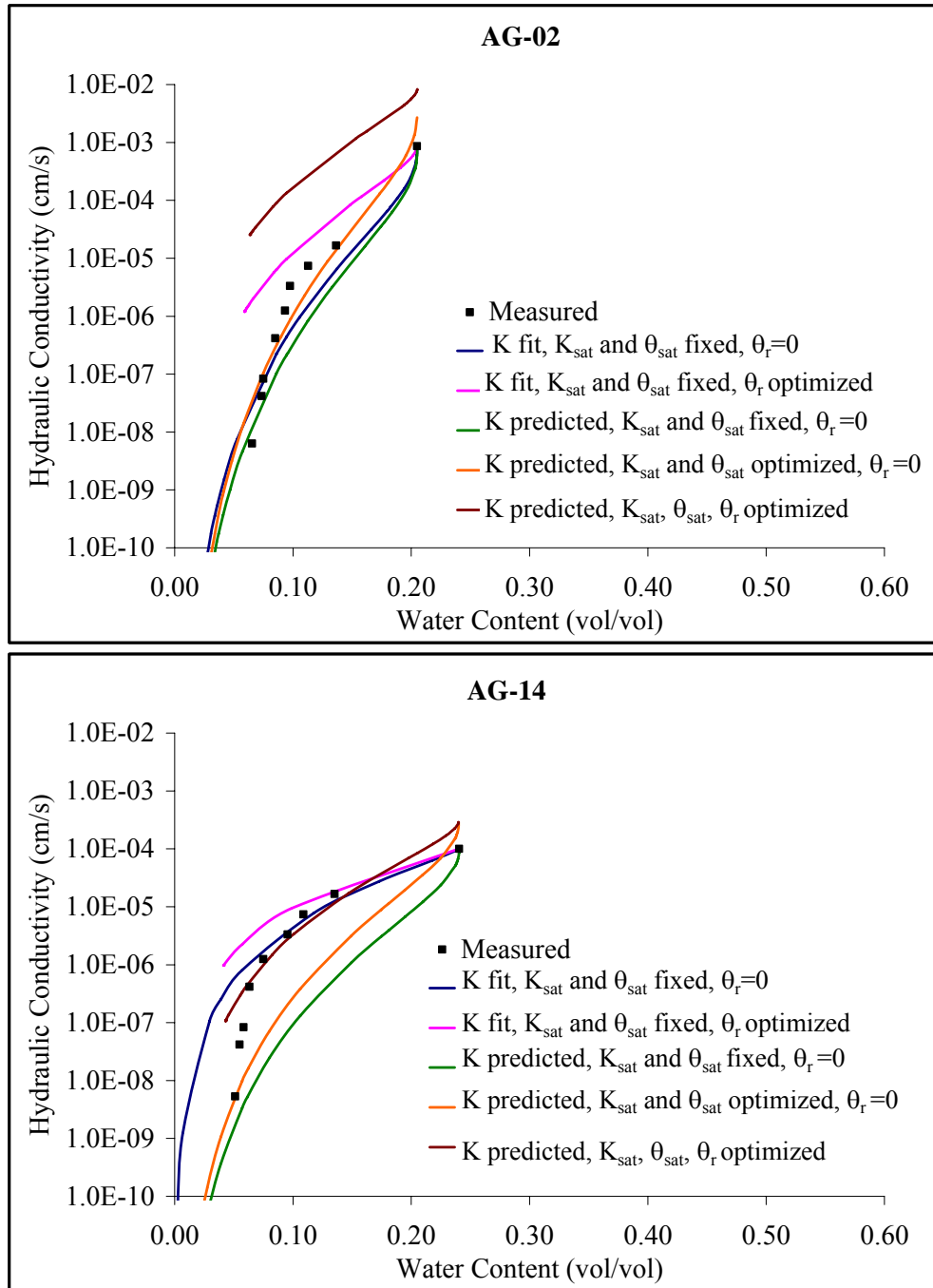
Figure 23. van Genuchten-Mualem fits (van Genuchten, 1980) to measured hydraulic conductivity data points and predictions of hydraulic conductivity for steady flow sites AG-02 and AG-14.
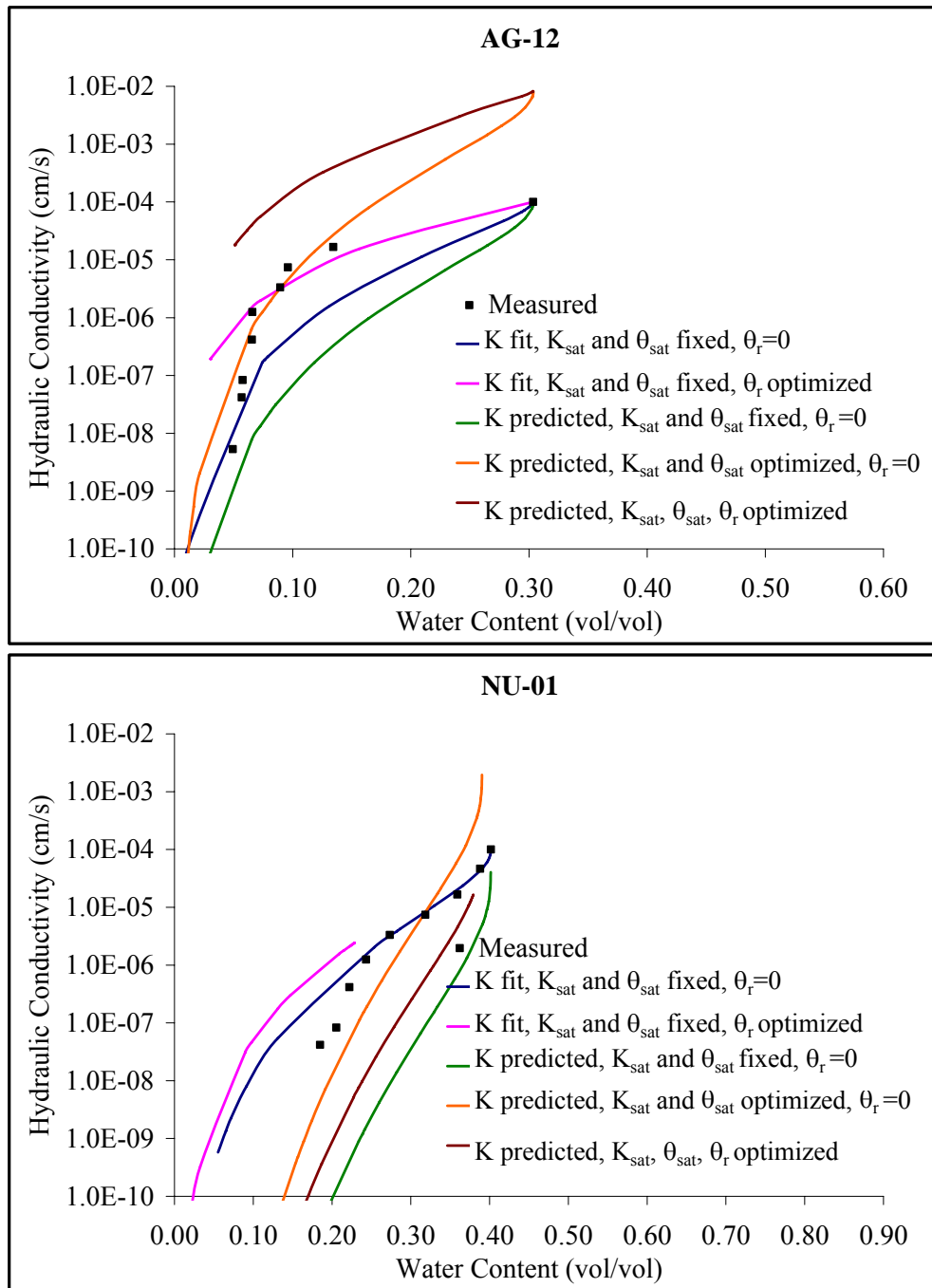
Figure 24. van Genuchten-Mualem fits (van Genuchten, 1980) to measured hydraulic conductivity data pointsand predictions of hydraulic conductivity for seasonally steady flow site AG-12 and unsteady flow site NU-01.

site NU-08 and unsteady flow site AG-15 due to the lack of water-retention data that are required by different fits and predictions.

Variations include:

- Simultaneous fit to measured $\theta(\psi)$ and $K(\theta)$ with K_{sat} and θ_{sat} fixed and $\theta_r = 0$
- Simultaneous fit to measured $\theta(\psi)$ and $K(\theta)$ with K_{sat} and θ_{sat} fixed and θ_r optimized
- Predicting $K(\theta)$ based on measured $\theta(\psi)$ with K_{sat} and θ_{sat} fixed and $\theta_r = 0$
- Predicting $K(\theta)$ based on measured $\theta(\psi)$ with K_{sat} and θ_{sat} fixed and θ_r optimized
- Predicting $K(\theta)$ based on measured $\theta(\psi)$ with K_{sat}, θ_{sat}, and θ_r optimized

In general, there is not a single variation among the fits and predictions that produces consistently better results than the others. When fitting the measured data points, results show that it is desirable to use known values for K_{sat} and θ_{sat} with θ_r set equal to zero. When predicting hydraulic conductivity, using known values for K_{sat} and θ_{sat} with θ_r set equal to zero and using optimized values of K_{sat}, θ_{sat}, and θ_r are the least good variations for these data.

Arya-Paris and van Genuchten-Mualem Predictions

Hydraulic parameters were predicted for each site based on detailed particle-size distributions of the core-sample material using a combination of the Arya-Paris pore-size distribution model (Arya and Paris, 1981) and vGM model (van Genuchten, 1980) as discussed above. Figures 25 and 26 show graphs of the Arya-Paris and vGM predicted
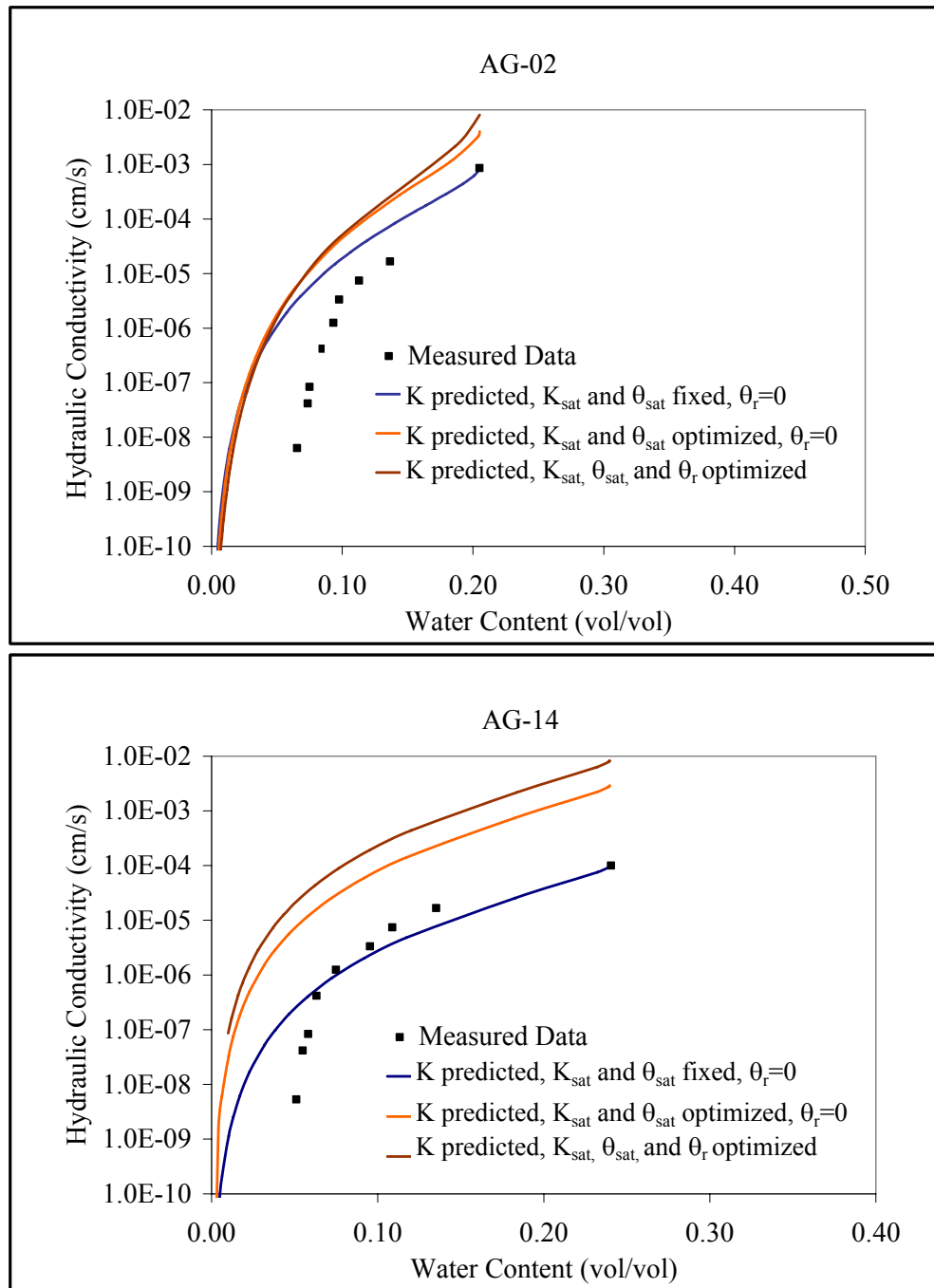
Figure 25. Laboratory-measured and Arya-Paris-van Genuchten-Mualem-predicted hydraulic conductivity curves for steady flow sites AG-02 (above) and AG-14 (below).

Figure 26. Laboratory-measured and Arya-Paris-van Genuchten-Mualem-predicted hydraulic conductivity curves for seasonally steady flow sites AG-12 (above) and NU-08 (below).

hydraulic conductivity curves. This approach does not systematically lead to over prediction or under prediction of hydraulic conductivity.

Rosetta Predictions

Hydraulic parameters were predicted using the Rosetta model for the sites with continuously or seasonally steady flow based on the bulk properties of the core samples (Table 7). The Rosetta model allows for different levels of information as input including as little as USDA texture or as much as known points on the $\theta(\psi)$ curve. There were three levels of complexity used for model inputs in this study, including 1) USDA texture only, 2) sand, silt, and clay percentages, and 3) sand, silt, and clay percentages and bulk density. Hydraulic conductivity curves (Figs. 27 and 28) are generated using the vGM model (van Genuchten, 1980) as discussed above. In all cases, the Rosetta parameters lead to prediction of hydraulic conductivity higher than that measured in the laboratory by the SSC method for any given water content.

Recharge Estimates

The data described above were used to predict aquifer recharge for the sites with continuously steady and seasonally steady flow, which are AG-02, AG-14, NU-08 and AG-12. Field water contents available for use in this study were measured during fall 1996, summer 2000, fall 2000, and spring 2001 (Figs. 5 and 6). For evaluation of seasonally steady sites, seasons are defined as 3-month periods where winter includes December through February, spring includes March through May, summer includes June

Table 7. Rosetta-predicted hydraulic property parameters based on input of USDA texture, texture class percentages, and texture class percentages plus bulk density.

| Site	Model Input	Θ_r	Θ_{sat}	α (1/cm)	n	K_{sat} (cm/s)
AG-02 6.1 m	Texture	0.053	0.375	0.0353	3.1798	7.44E-03
	% Sand, Silt, Clay	0.048	0.381	0.0363	3.4727	8.70E-03
	% Sand, Silt, Clay and Bulk Density	0.047	0.328	0.0343	3.3477	6.13E-03
AG-12 4.9 m	Texture	0.053	0.375	0.0353	3.1798	7.44E-03
	% Sand, Silt, Clay	0.043	0.385	0.0399	2.5422	3.62E-03
	% Sand, Silt, Clay and Bulk Density	0.045	0.387	0.0381	2.6251	4.42E-03
AG14 5.5 m	Texture	0.053	0.375	0.0353	3.1798	7.44E-03
	% Sand, Silt, Clay	0.050	0.379	0.0352	3.716	1.06E-02
	% Sand, Silt, Clay and Bulk Density	0.050	0.345	0.0325	3.7077	8.87E-03
NU-08 5.5 m	Texture	0.053	0.375	0.0353	3.1798	7.44E-03
	% Sand, Silt, Clay	0.044	0.384	0.0394	2.8007	4.73E-03
	% Sand, Silt, Clay and Bulk Density	0.043	0.306	0.0389	2.6551	2.52E-03
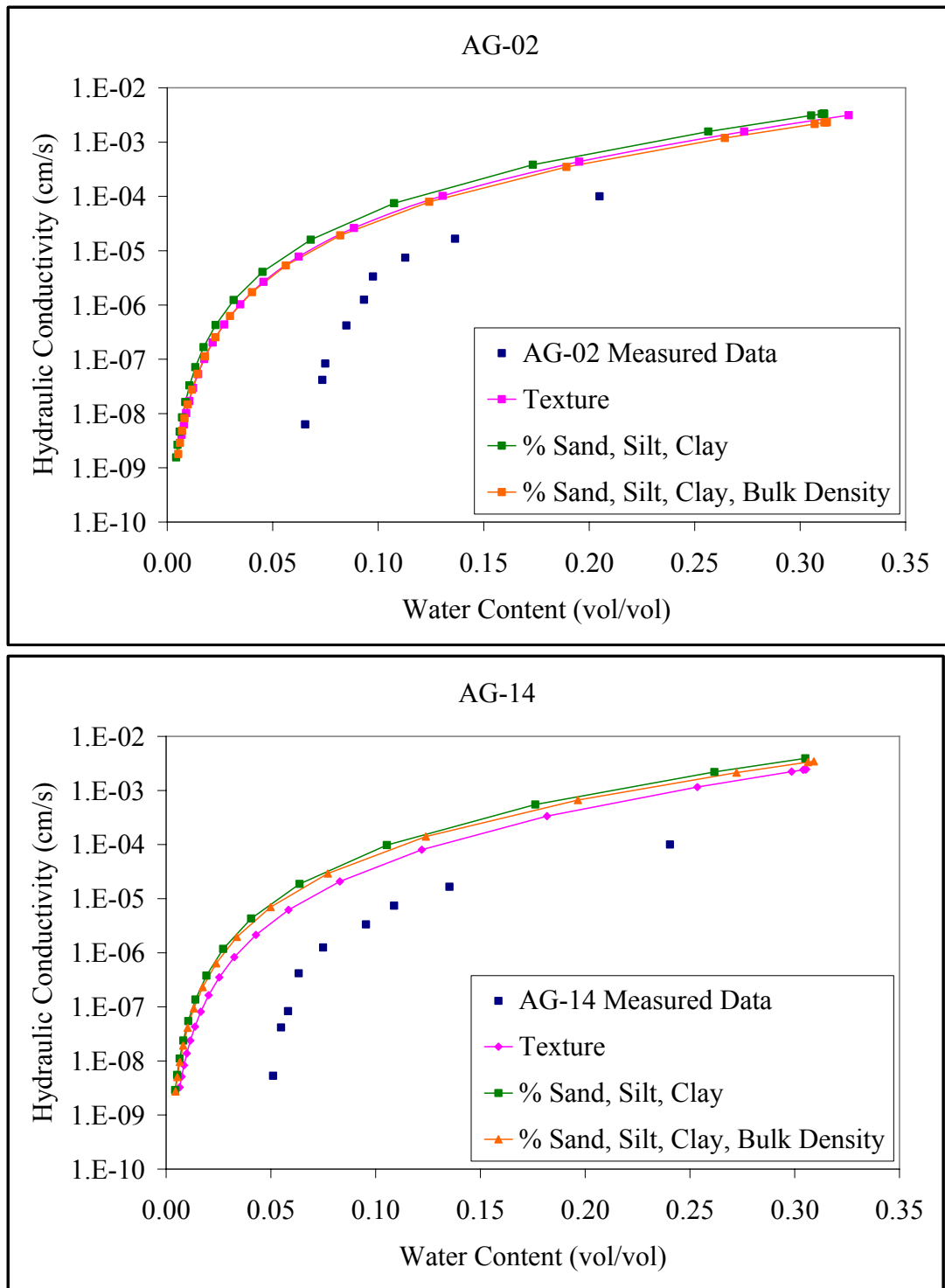
Figure 27. Laboratory-measured and Rosetta-predicted hydraulic conductivity curves for steady flow sites AG-02 (above) and AG-14 (below). Model inputs are texture, % sand, silt, clay, or % sand, silt, clay, and bulk density.
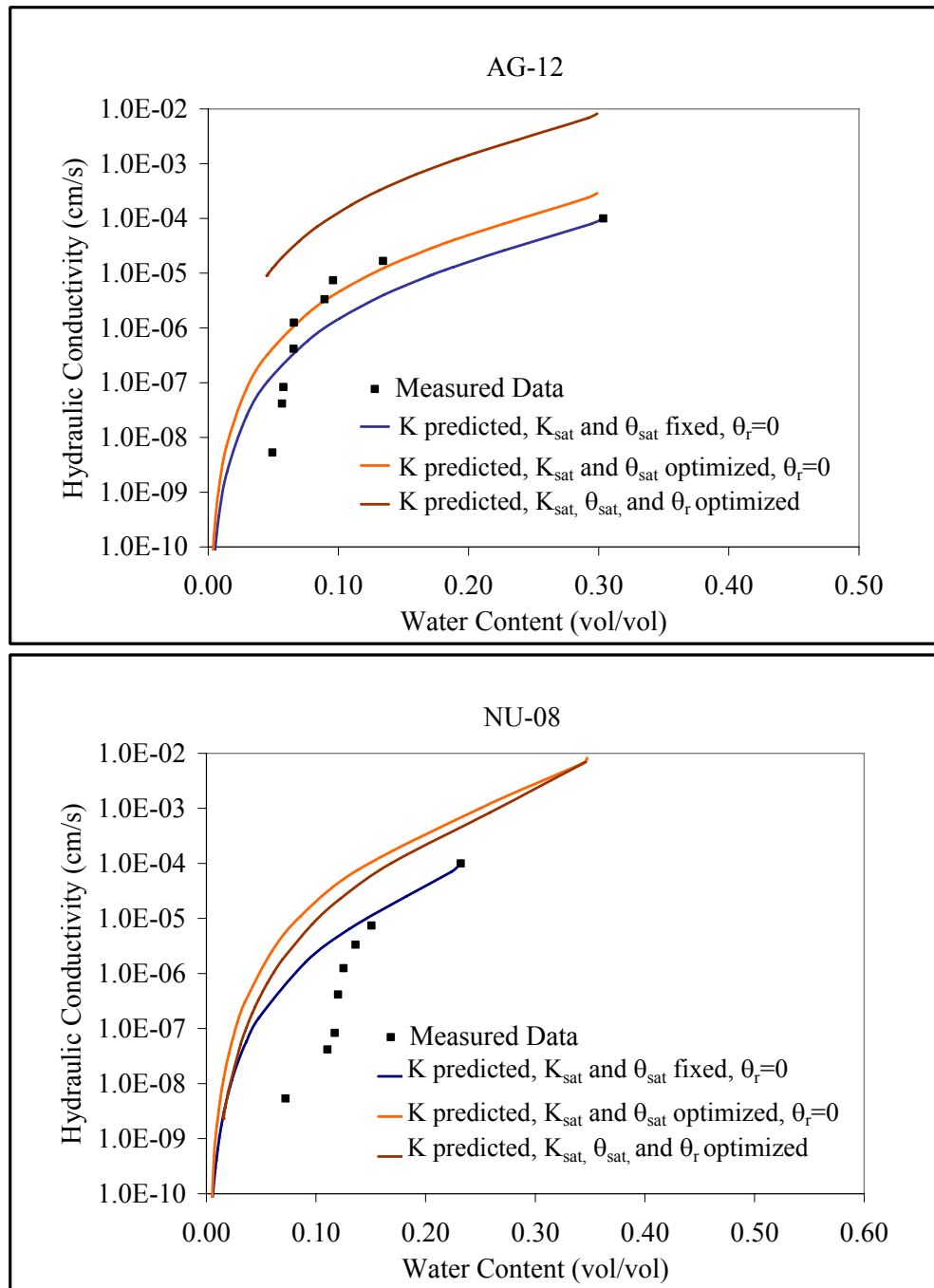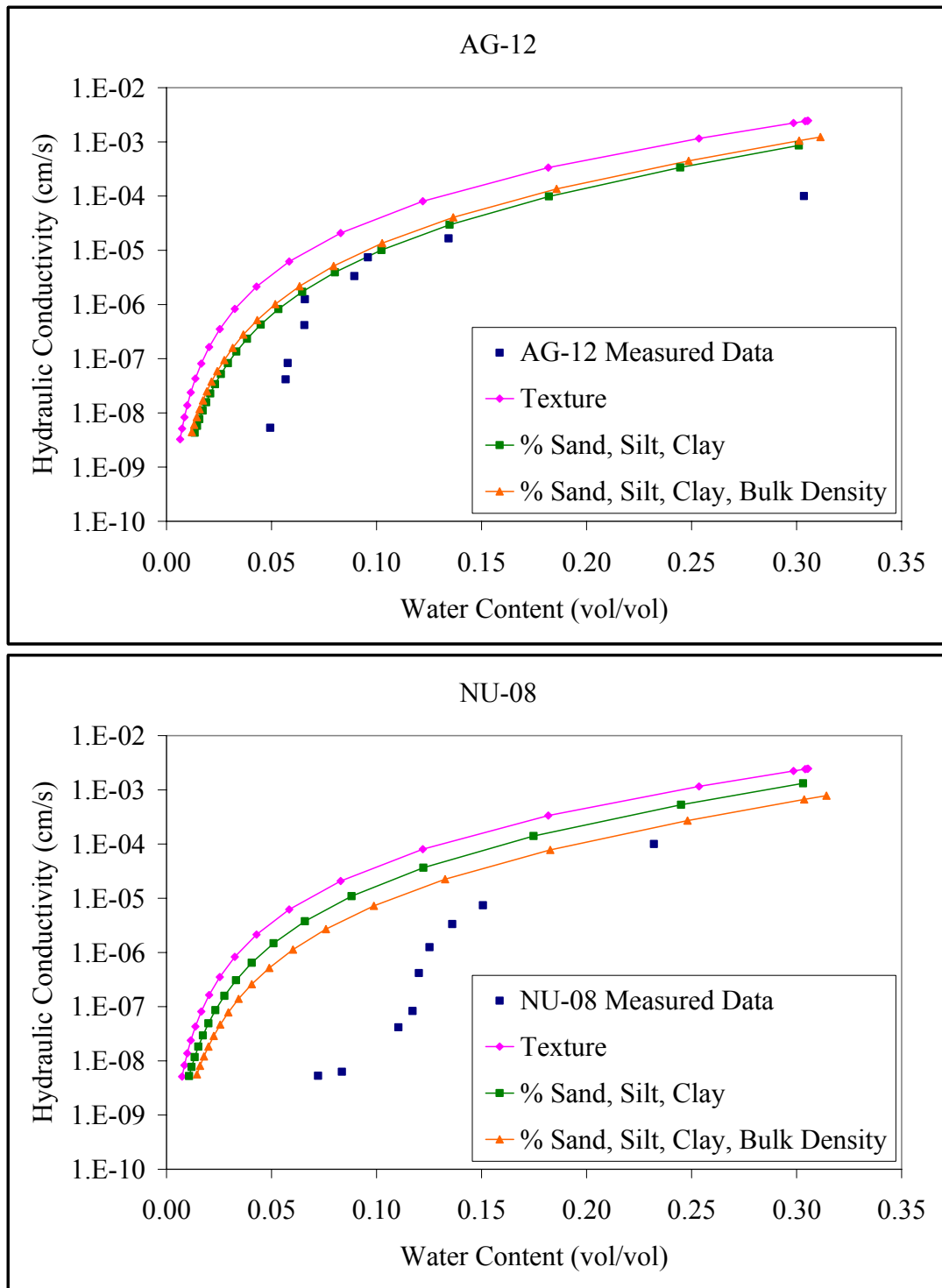
Figure 28. Laboratory-measured and Rosetta-predicted hydraulic conductivity curves for seasonally steady flow sites AG-12 (above) and NU-08 (below). Model inputs are texture, % sand, silt, clay, or % sand, silt, clay, and bulk density.

through August, and fall includes September through November. Even for sites considered to be continuously steady, there is some small variation in the water-content profiles over time either due to measurement error or real variation in water content.

Recharge estimates were therefore calculated for the lowest and highest water-content values for comparison. Tables 8, 9, 10, and 11 summarize the recharge estimates by site for the continuously steady and seasonally steady regimes. With all variations of the 6 main methods used there are 13 estimates total (Table 2) as well as the K value associated with the measured maximum and minimum water content (for steady flow sites) or seasonal water content (for seasonally steady flow sites) and the recharge as a percentage of rainfall for the corresponding year or season.

Water Table Fluctuations

The change in height of the water table over time between the rising limb and the estimated recession curve was determined by taking the difference between the measured water level and the predicted water level. The predicted water level is calculated based on a decline rate taken from the estimated recession curve and therefore includes the time factor required in the recharge calculation as described above. Where this difference is positive, it is assumed that recharge is occurring. Where values are negative it is assumed that no recharge is occurring. Table 12 shows the data used in recharge calculations for 2001 as an example. Water table fluctuations appear to occur on a seasonal basis over the area examined here. Recharge rates were calculated by year and by season for the period from spring 1997 through summer 2001 (Fig. 29). Yearly

Table 8. Annual Darcian recharge estimates for continuously steady flow site AG-02. Values were calculated for the maximum (0.095) and minimum (0.086) volumetric field water contents measured over time. Precipitation was 120.93 cm for the year of maximum water content and 94.03 cm for the year of the minimum water content.

Method	Parameters	Hydraulic conductivity (cm/s), max. and min.	Recharge rates (cm/y), max. and min.	% of rainfall that becomes recharge, max. and min.
van Genuchten-Mualem simultaneous fit to measured K and water retention	K_{sat} fixed θ_{sat} fixed $\theta_r=0$	4.38E-07 2.25E-07	13.8 7.1	11.4 % 7.8 %
	K_{sat} fixed θ_{sat} fixed θ_r optimzed	9.74E-06 6.38E-06	307.2 201.2	254.0 % 221.0 %
van Genuchten-Mualem fit to measured water retention with K predicted	K_{sat} fixed θ_{sat} fixed $\theta_r=0$	2.16E-07 1.01E-07	6.8 3.2	5.6 % 3.4 %
	K_{sat} optimized θ_{sat} optimized $\theta_r=0$	5.71E-07 4.34E-07	18.0 13.7	14.9 % 14.6 %
	K_{sat} optimized θ_{sat} optimized θ_r optimized	1.34E-04 9.02E-05	4215.8 2843.1	3486.1 % 3023.6 %
van Genuchten-Mualem fit to Arya-Paris-predicted water retention with K predicted	K_{sat} fixed θ_{sat} fixed $\theta_r=0$	1.50E-05 1.02E-05	472.9 321.1	391.1 % 341.5 %
	K_{sat} optimized θ_{sat} optimized $\theta_r=0$	3.50E-05 2.10E-05	1104 662	912.9 % 704.0 %
	K_{sat} optimized θ_{sat} optimized θ_r optimized	3.58E-05 2.44E-05	1128 770	932.8 % 818.9 %
Power law fit to measured K data	N/A	8.66E-07 3.04E-07	27.3 9.6	22.6 % 10.2 5
Hand interpolation of K data	N/A	1.60E-06 4.19E-07	50.5 13.2	41.8 % 14.0 %
Rosetta parameters to estimate water retention and K	Texture only	3.30E-05 2.38E-05	1040.7 749.9	860.6 % 797.5 %
	% Sand, % silt, % clay	4.84E-05 3.51E-05	1526.3 1106.9	1262.1 % 1177.2 %
	% Sand, % silt, % clay, and bulk density	3.20E-05 1.91E-05	1009.2 602.3	834.5 % 640.5 %

Table 9. Annual Darcian recharge estimates for continuously steady flow site AG-14. Values were calculated for the maximum (0.057) and minimum (0.039) field water contents measured over time. Precipitation was 120.93 cm for the year of maximum water content and 91.03 cm for the year of the minimum water content.

Method	Parameters	Hydraulic conductivity (cm/s), max. and min.	Recharge rates (cm/y), max. and min.	% of rainfall that becomes recharge, max. and min.
van Genuchten-Mualem simultaneous fit to measured K and water retention	K_{sat} fixed θ_{sat} fixed $\theta_r=0$	8.05E-07 2.54E-07	25.4 8.0	21.0 8.5
	K_{sat} fixed θ_{sat} fixed θ_r optimzed	2.24E-06 3.17E-14	70.6 0.0	58.4 0.0
van Genuchten-Mualem fit to measured water retention with K predicted	K_{sat} fixed θ_{sat} fixed $\theta_r=0$	3.17E-09 3.17E-10	0.1 0.0	0.1 0.0
	K_{sat} optimized θsat optimized $\theta_r=0$	9.51E-09 9.51E-10	0.3 0.0	0.2 0.0
	K_{sat} optimized θsat optimized θ_r optimized	3.33E-07 3.17E-13	10.5 0.0	8.7 0.0
van Genuchten-Mualem fit to Arya-Paris-predicted water retention with K predicted	K_{sat} fixed θ_{sat} fixed $\theta_r=0$	3.87E-07 1.08E-07	12.2 3.4	10.1 3.6
	K_{sat} optimized θ_{sat} optimized $\theta_r=0$	1.13E-05 3.09E-06	356.4 97.45	294.7 103.6
	K_{sat} optimized θ_{sat} optimized θ_r optimized	3.23E-05 8.78E-06	1017.1 276.9	841.1 294.5
Power law fit to measured K data	N/A	4.76E-08 3.17E-09	1.5 0.1	1.2 0.1
Hand interpolation of K data	N/A	2.85E-08 3.17E-12	0.9 0.0	0.7 0.0
Rosetta parameters to estimate water retention and K	Texture only	5.89E-06 1.57E-06	185.8 49.5	153.6 52.6
	% Sand, % silt, % clay	1.31E-05 3.83E-06	413.1 120.8	341.6 128.5
	% Sand, % silt, % clay, and bulk density	1.09E-05 3.17E-06	343.7 100.0	284.2 106.3

Table 10. Seasonal Darican recharge estimates for seasonally steady flow site
AG-12. Seasonal water contents were 0.073 for fall 1996, 0.079 for summer 2000,
0.065 for fall 2000, and 0.074 for spring 2001. Rainfall was 29.82 cm for summer 1996,
37.21 cm for summer 2000, 30.40 cm for fall 2000, and 33.06 cm for spring 2001.
Recharge rates and % of rainfall values are in order by time starting with fall 1996.

Method	Parameters	Hydraulic conductivity (cm/s)	Season	Recharge Rates (cm/y)	% of rainfall (recharge rate x 0.25)
van Genuchten-Mualem simultaneous fit to measured K and retention	K_{sat} fixed θ_{sat} fixed $\theta_r=0$	1.55E-07 2.14E-07 1.00E-07 1.68E-07	Fall 1996 Summer 2000 Fall 2000 Spring 2001	4.9 6.7 3.2 5.3	4.1 4.5 2.6 3.9
	K_{sat} fixed θ_{sat} fixed θ_r optimzed	2.10E-06 2.48E-06 1.47E-06 1.97E-06	Fall 1996 Summer 2000 Fall 2000 Spring 2001	66.2 78.13 46.3 62.2	55.5 52.5 38.1 46.2
van Genuchten-Mualem fit to measured retention with K predicted	K_{sat} fixed θ_{sat} fixed $\theta_r=0$	1.59E-08 2.06E-08 7.61E-09 1.27E-08	Fall 1996 Summer 2000 Fall 2000 Spring 2001	0.5 0.65 0.2 0.4	0.4 0.4 0.2 0.3
	K_{sat} optimized θ_{sat} optimized $\theta_r=0$	1.05E-06 1.71E-06 6.26E-07 1.23E-06	Fall 1996 Summer 2000 Fall 2000 Spring 2001	33.2 53.9 19.7 38.8	27.8 36.2 16.2 28.8
	K_{sat} optimized θ_{sat} optimized θ_r optimized	5.60E-05 7.29E-05 3.95E-05 5.98E-05	Fall 1996 Summer 2000 Fall 2000 Spring 2001	1764.6 2299.7 1246.1 1886.4	1479.4 1545.1 1024.7 1401.1
van Genuchten-Mualem fit to Arya-Paris-predicted retention with K predicted	K_{sat} fixed θ_{sat} fixed $\theta_r=0$	4.95E-07 6.56E-07 3.41E-07 5.33E-07	Fall 1996 Summer 2000 Fall 2000 Spring 2001	15.6 20.7 10.8 16.8	13.1 13.9 8.8 12.5
	K_{sat} optimized θ_{sat} optimized $\theta_r=0$	1.55E-06 2.04E-06 1.07E-06 1.67E-06	Fall 1996 Summer 2000 Fall 2000 Spring 2001	48.9 64.4 33.8 52.6	41.0 43.3 27.8 39.1
	K_{sat} optimized θ_{sat} optimized θ_r optimized	4.45E-05 5.88E-05 3.08E-05 4.76E-05	Fall 1996 Summer 2000 Fall 2000 Spring 2001	1402.2 1855.0 970.8 1500.7	1175.6 1246.3 798.4 1114.6
Power law fit to measured K data	N/A	4.92E-07 9.04E-07 2.16E-07 5.74E-07	Fall 1996 Summer 2000 Fall 2000 Spring 2001	15.5 28.5 6.8 18.1	13.0 19.1 5.6 13.4
Hand interpolation of K data	N/A	1.80E-06 2.50E-06 1.60E-06 2.00E-06	Fall 1996 Summer 2000 Fall 2000 Spring 2001	56.8 78.8 50.5 63.1	47.6 52.9 41.5 46.9

Table 10. Continued

Method	Parameters	Hydraulic conductivity (cm/s)	Season	Recharge Rates (cm/y)	% of rainfall (recharge rate x 0.25)
Rosetta parameters to estimate retention and K	Texture only	1.33E-05	Fall 1996	419.0	351.3
		1.79E-05	Summer 2000	565.2	379.7
		9.03E-06	Fall 2000	284.9	234.3
		1.43E-05	Spring 2001	451.2	335.1
	% Sand, %silt, %clay	2.72E-06	Fall 1996	85.8	71.9
		3.77E-06	Summer 2000	118.9	79.9
		1.79E-06	Fall 2000	56.3	46.3
		2.94E-06	Spring 2001	92.6	68.8
	% Sand, %silt, %clay, and bulk density	3.68E-06	Fall 1996	116.1	97.3
		5.05E-06	Summer 2000	159.1	106.9
		2.43E-06	Fall 2000	76.6	63.0
		4.00E-06	Spring 2001	126.1	93.7

Table 11. Seasonal Darcian recharge estimates for seasonally steady flow site NU-08. Seasonal water contents were 0.117 for fall 1996, .080 for summer 2000, 0.119 for fall 2000, and 0.136 for spring 2001. Rainfall was 29.82 cm for summer 1996, 37.21 cm for summer 2000, 30.40 cm for fall 2000, and 33.06 cm for spring 2001. Recharge rates and % of rainfall values are in order by time starting with fall 1996.

Method	Parameters	Hydraulic conductivity (cm/s)	Season	Recharge Rates (cm/y)	% of rainfall (recharge rate x 0.25)
van Genuchten-Mualem simultaneous fit to measured K and retention	K_{sat} fixed θ_{sat} fixed $\theta_r=0$	No retention data available	N/A	N/A	N/A
	K_{sat} fixed θ_{sat} fixed θ_r optimzed	No retention data available	N/A	N/A	N/A
van Genuchten-Mualem fit to measured retention with K predicted	K_{sat} fixed θ_{sat} fixed $\theta_r=0$	No retention data available	N/A	N/A	N/A
	K_{sat} optimized θ_{sat} optimized $\theta_r=0$	No retention data available	N/A	N/A	N/A
	K_{sat} optimized θ_{sat} optimized θ_r optimized	No retention data available	N/A	N/A	N/A

Table 11. Continued

Method	Parameters	Hydraulic conductivity (cm/s)	Season	Recharge Rates (cm/y)	% of rainfall (recharge rate x 0.25)
van Genuchten-Mualem fit to Arya-Paris-predicted retention with K predicted	K_{sat} fixed θ_{sat} fixed $\theta_r=0$	4.19E-06 9.98E-07 4.44E-06 7.64E-06	Fall 1996 Summer 2000 Fall 2000 Spring 2001	132.1 31.5 140.9 240.9	110.7 21.1 115.1 178.9
	K_{sat} optimized θ_{sat} optimized $\theta_r=0$	3.80E-05 7.91E-06 4.04E-05 7.24E-05	Fall 1996 Summer 2000 Fall 2000 Spring 2001	1198.4 249.5 1274.1 2283.2	1004.7 167.6 1047.7 1695.8
	K_{sat} optimized θ_{sat} optimized θ_r optimized	3.75E-05 1.97E-05 1.86E-05 3.25E-06	Fall 1996 Summer 2000 Fall 2000 Spring 2001	1183.4 621.3 585.7 102.5	992.1 417.4 481.7 76.1
Power law fit to measured K data	N/A	3.14E-07 6.34E-09 3.68E-07 1.51E-06	Fall 1996 Summer 2000 Fall 2000 Spring 2001	9.9 0.2 11.6 47.7	8.3 0.1 9.5 35.4
Hand interpolation of K data	N/A	1.90E-07 0.00E+00 3.01E-07 3.34E-06	Fall 1996 Summer 2000 Fall 2000 Spring 2001	6.0 0.0 9.5 105.2	5.0 0.0 7.8 78.1
Rosetta parameters to estimate retention and K	Texture only	6.91E-05 1.77E-05 7.31E-05 1.20E-04	Fall 1996 Summer 2000 Fall 2000 Spring 2001	2179.1 558.2 1205.3 3784.3	1826.9 375.0 1895.8 2810.7
	% sand %silt %clay	3.08E-05 7.40E-06 3.27E-05 5.51E-05	Fall 1996 Summer 2000 Fall 2000 Spring 2001	971.3 233.4 1031.2 1737.6	814.3 156.8 848.1 1290.6
	% sand %silt %clay bulk density	1.38E-05 3.23E-06 1.46E-05 2.49E-05	Fall 1996 Summer 2000 Fall 2000 Spring 2001	435.2 101.9 460.4 785.3	364.9 68.4 378.6 583.2

Table 12. Example of recharge estimation data from well AG-02 for 2001.
Predicted water level is from the antecedent recession curves based on an exponential
decay function applied to the measured falling limb data (S_y: specific yield).

| Date of measurement	Cumulative time (days)	Observed water level (m)	Predicted water level (m)	Observed – predicted (cm)	Recharge (cm) = S_y(observed-predicted)
1/20/2001	22	34.64	34.60	3.41	0.92
2/1/2001	34	34.67	34.60	6.36	1.72
3/1/2001	62	34.88	34.56	32.12	8.67
4/2/2001	94	35.08	34.75	33.24	8.97
5/30/2001	123	35.38	34.94	44.49	12.01
6/17/2001	141	35.36	35.29	7.15	1.93
7/31/2001	185	35.35	35.14	20.93	5.65
8/31/2001	216	35.23	35.21	1.46	0.39
9/30/2001	246	35.06	35.10	-4.39	0.00
10/31/2001	277	34.87	34.95	-7.44	0.00
11/30/2001	307	34.71	34.78	-6.73	0.00
12/31/2001	338	34.58	34.63	-4.52	0.00
				Total	40.27
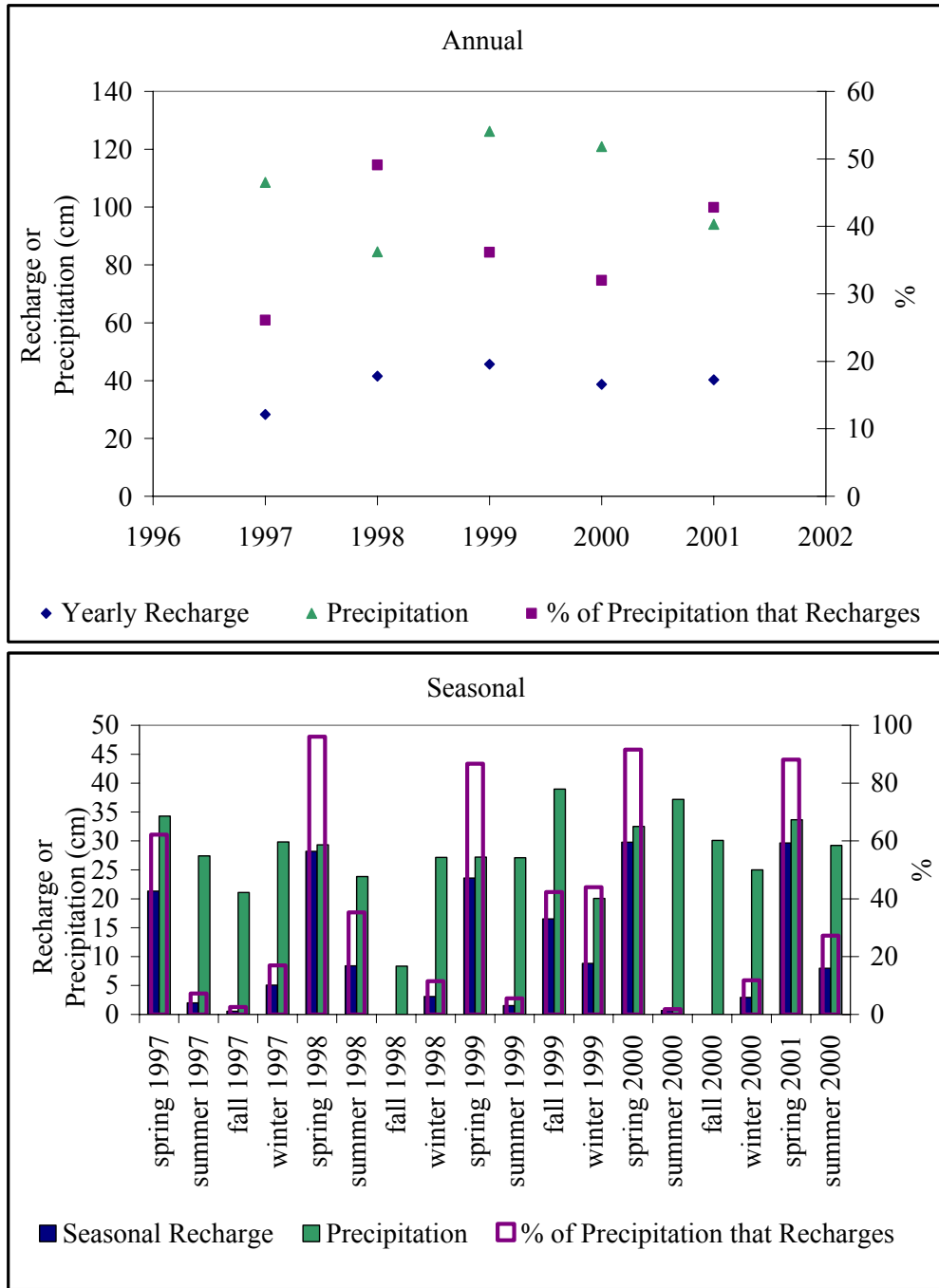
Figure 29. Annual (above) and seasonal (below) recharge as estimated by the water-table fluctuation method for well AG-02. Percentage of precipitation that recharges is calculated by dividing recharge by precipitation for the given period.

values range from 28.3 to 45.7 cm. Relative to precipitation, the values range from 26 to

46 percent. Average seasonal recharge values for the period of record are 22.1 cm, 3.8

cm, 3.1 cm, and 4.0 cm for spring, summer, fall, and winter respectively. Relative to

precipitation the values are 85.0, 15.5, 11.2, and 21.1 percent for spring, summer, fall,

and winter respectively.

Steady Flow Evaluation with VS2DT

Numerical simulations were run in order to assess the steadiness of flow at site

AG-02 for the period of October 6, 2000 to March 12, 2001. This site was chosen

because hydraulic properties were measured at two depths, one within and one above the

region of steady flow. The simulation period was chosen because 1) field water contents

were measured on the first and last day of the simulation period, 2) the simulation period

includes mainly the time of year when ET is negligible and can therefore be ignored, 3)

precipitation data were available for the entire period, and 4) the period was sufficiently

short that precipitation data could be prescribed on a daily basis.

The model did produce a zone of steady flow in the region where field-water

contents indicate that steady flow occurs. The steady-flow region occurs between the

depths of 5 and 6 m. Water-content changes occurred above and below this region only,

therefore water must have moved through this region without changing the water content

(Fig. 30). Water-content changes below the zone of steady flow are due to the rising

water table. Modeled water contents are much higher than the measured water contents

in the upper profile. Although ET is considered minimal during the winter season, there

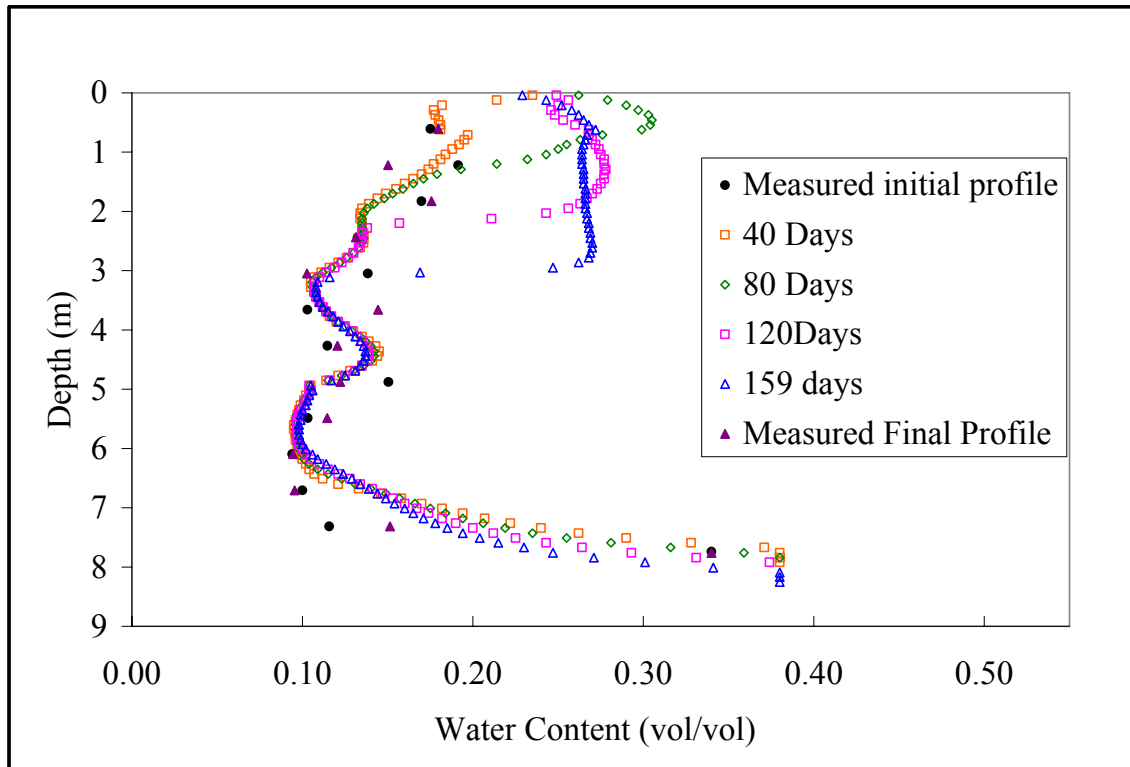Figure 30. VS2DT model results for steady-flow evaluation of site AG-02 for the period of October 06, 2000 to March 12, 2001. A zone of steady flow occurs between 5 and 6 m. The graph shows model output at various times throughout the simulation period.

may have been significant ET occurring during the early and late parts of the simulation

period, or it may have been a warmer than average winter.

ERROR ANALYSIS

Recharge rates calculated directly from laboratory-measured hydraulic-conductivity and field-water contents contain some error. Error in hydraulic-conductivity data measured using the SSC method could arise due to uncertainty in run parameters including inflow rate and centrifugal driving force. According to the manufacturer of the metering pumps used in this study (3M Micro Infusion AVI pumps), error in inflow rate is +/-2.0 percent. The error in rotational speed for the Beckman Model J-6M centrifuge is +/- 20 rpm. Figure 31 shows the negligible effect of these possible errors on the hydraulic-conductivity curve. Table 13 shows the translation of the error in K to recharge rate.

Error in field-water content determined by replicate samples by USGS New Jersey District personnel was estimated to be +/- 10 percent on average (Baehr, 2002, personal communication). This is the most significant error when translated into recharge rates, especially where the field-water content corresponds with a hydraulic conductivity value that is on the steep portion of the $K(\theta)$ curve. The effect of this error on $K(\theta)$ and on recharge rate was evaluated for the steady and seasonally steady flow sites. The field-water content used in this evaluation is that determined at the time the cores were collected for measurement of hydraulic properties. The results are given in Table 14 and shown graphically in Figures 32 and 33. This analysis, discussed below, illustrates the importance of the determination of field-water content for use in Darcian recharge estimates.
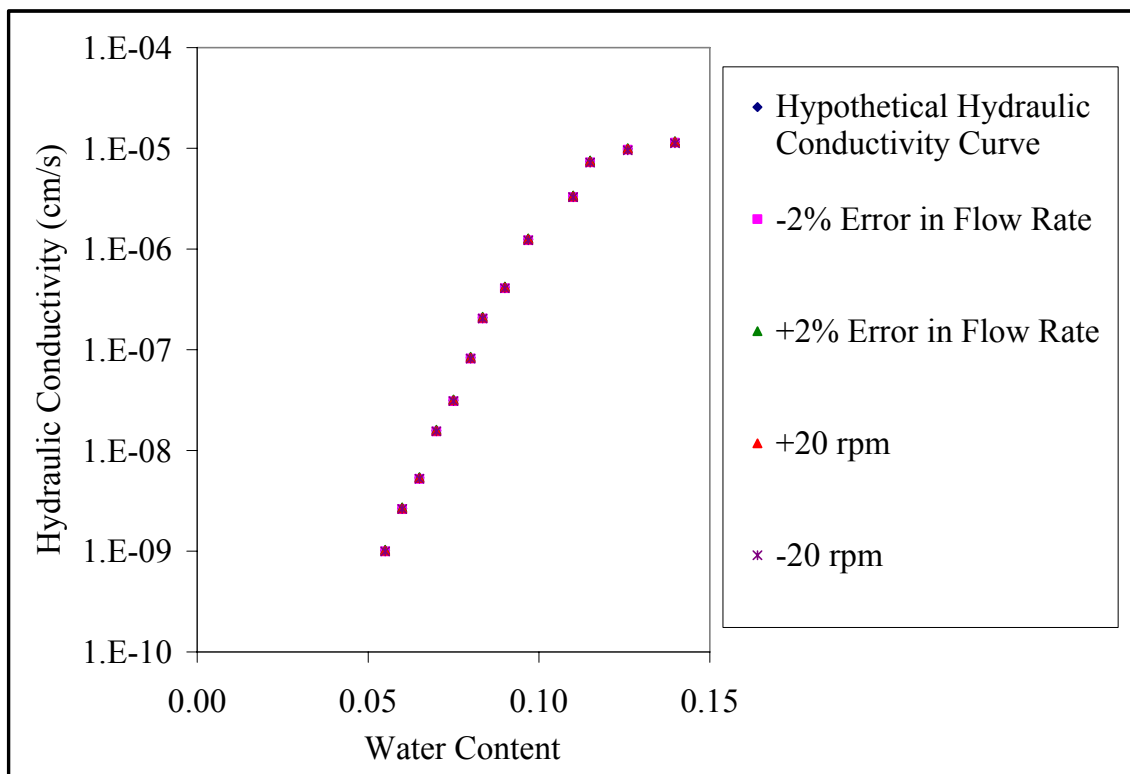
Figure 31. Graph of possible error in hydraulic conductivity due to mechanical uncertainty of +/-2% in inflow rate and +/-20 rpm in centrifuge speed. All five values print essentially on top of each other at this scale. Data used here are hypothetical, which allows for the entire range of measurable hydraulic conductivity to be evaluated. Real data do not generally span the entire range.

Table 13. Effect of the mechanical error associated with the measurement of unsaturated hydraulic conductivity on recharge rate.

Recharge Rate Based on Hypothetical K (cm/y)	Recharge Rate With - 2% Error in Flow Rate (cm/y)	Recharge Rate With + 2% Error in Flow Rate (cm/y)	Recharge Rate With - 20 rpm Driving Force (cm/y)	Recharge Rate With + 20 rpm Driving Force (cm/y)
105.14	103.04	107.24	107.28	103.07
39.43	38.64	40.22	40.23	38.65
13.14	12.88	13.41	13.41	12.88
6.57	6.44	6.70	6.70	6.44
2.63	2.58	2.68	2.68	2.58
0.99	0.97	1.01	1.01	0.98
0.50	0.49	0.51	0.51	0.49
0.17	0.16	0.17	0.17	0.17
0.08	0.08	0.09	0.09	0.08
0.03	0.03	0.03	0.03	0.03

Table 14. Effect of an error of +/- 10% in field-water content on recharge estimates based on hand interpolation of measured hydraulic-conductivity data for steady-flow sites AG-02 and AG-14 and seasonally steady flow sites NU-08 and AG-12.

	AG-02	AG-14	AG-12	NU-08
Field-water content (vol/vol)	0.093	0.049	0.074	0.117
Recharge rate at field-water content (cm/y)	37.8	0.1	56.8	12.6
Field-water content (vol/vol) +10%	0.102	0.054	0.081	0.129
Recharge rate at field-water content +10% (cm/y)	78.8	0.4	69.4	44.2
Field-water content (vol/vol) -10%	0.084	0.044	0.067	0.105
Recharge rate at field-water content -10% (cm/y)	6.3	0.0	28.4	0.2

Figure 32. Effect of +/-10% error in measured field-water content (θ) on recharge rates based on hand-interpolated hydraulic conductivity data for steady flow sites AG-02 and AG-14. The vertical arrows indicate the water content measured at the time of sample collection and the water contents resulting from +/- 10% error.
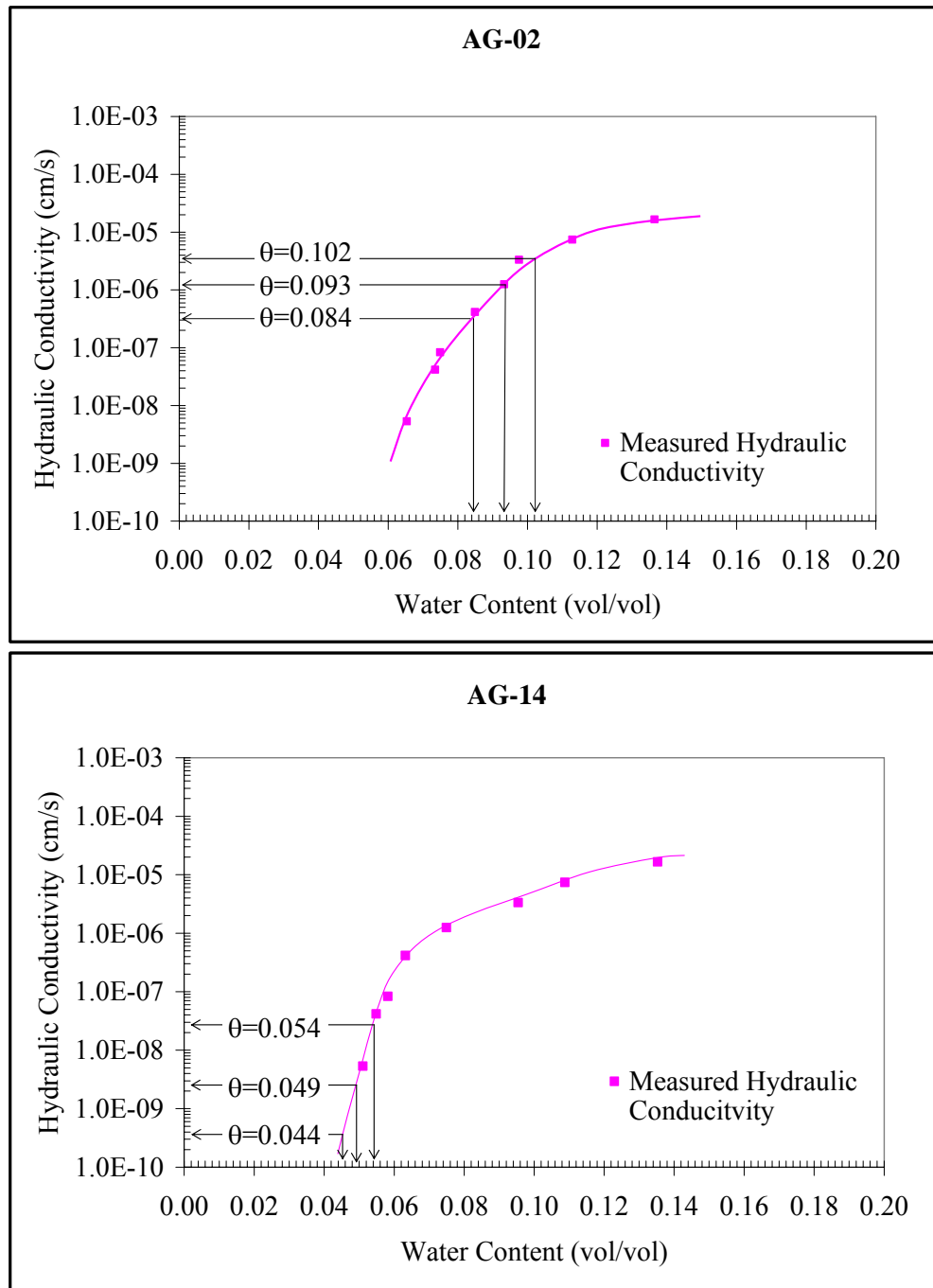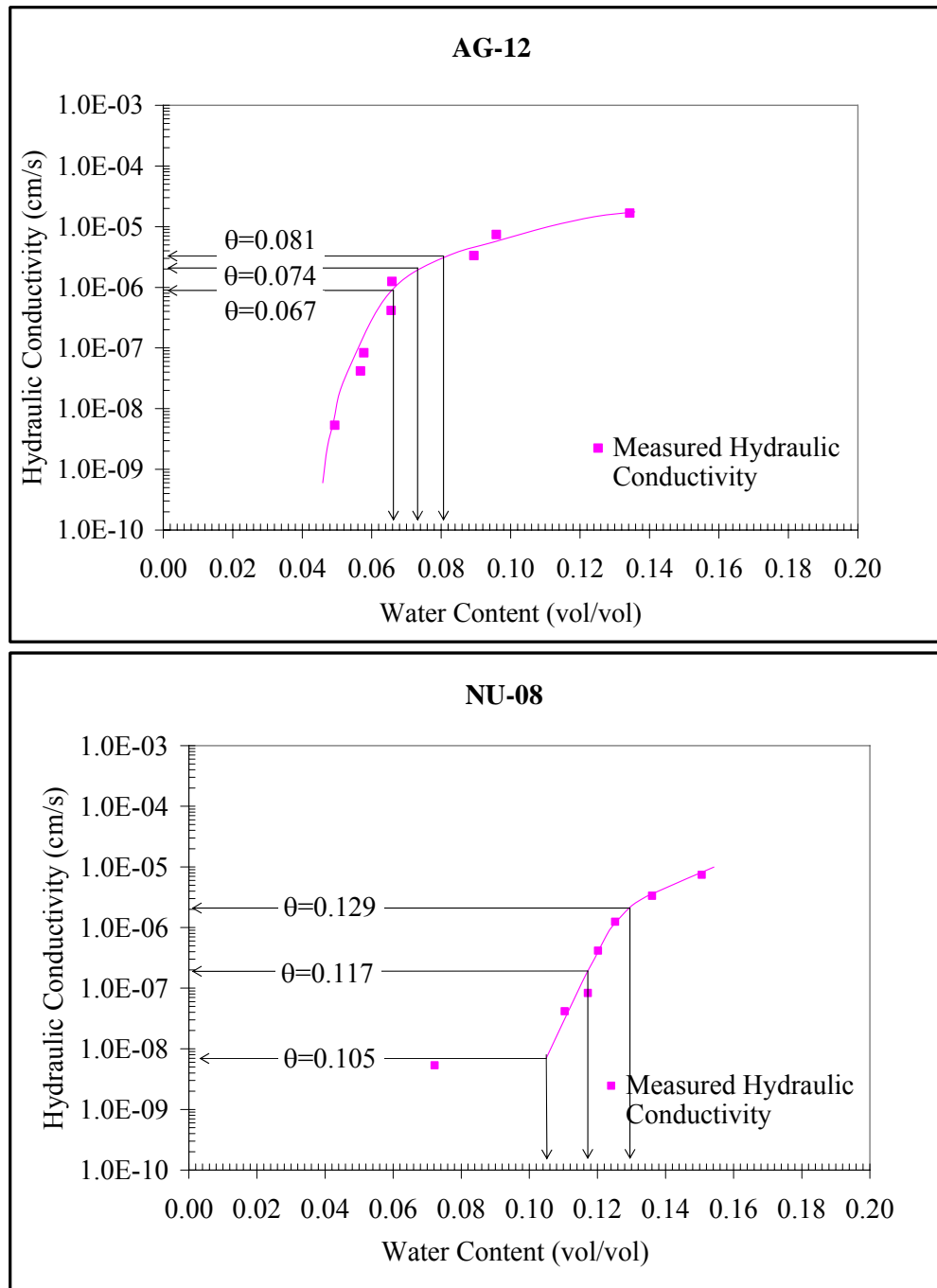
Figure 33. Effect of +/-10% error in measured field-water content (θ) on recharge rates based on hand-interpolated hydraulic conductivity data for seasonally steady flow sites AG-12 and NU-08. The vertical arrows indicate the water content measured at the time of sample collection and the water contents resulting from +/- 10% error.

DISCUSSION

Interpolation of Unsaturated Hydraulic Conductivity

Results show that, although reasonable estimates come from directly measured unsaturated hydraulic conductivity, the goodness of fit associated with the method of curve fitting is critical because of the highly non-linear relationship between hydraulic conductivity and water content. Goodness of fit is extremely important if the range of water content observed in the field occurs within the steep part of the curve where very small changes in water content result in large differences in conductivity and therefore recharge rate. Even a relatively good visual fit can lead to unreasonable recharge values. A hand interpolation of the data points, and in many cases a simple power-law fit, yielded reasonable results for all data, whereas the commonly-used vGM-curve fits in some cases resulted in recharge values greater than 200 percent of annual precipitation (Tables 8-11). In the following discussion of predicted recharge rates, comparisons will be made with values based on the hand interpolation of unsaturated hydraulic-conductivity data.

Prediction of Unsaturated Hydraulic Conductivity

It is desirable to estimate unsaturated hydraulic conductivity from easily measured properties, for example water retention or particle-size distributions. Measured water-retention data were used to predict unsaturated hydraulic conductivity with the vGM model with the K_{sat}, θ_{sat}, and θ_r parameters (described above) being fixed or optimized. The best predictions of hydraulic conductivity for AG-02 and AG-12 resulted when K_{sat}

and θ_{sat} were optimized and θ_r was set equal to zero (Figs. 23 and 24). For AG-14, optimization of all parameters yielded the best fit (Fig. 23). In some cases, there is at least one hydraulic conductivity curve that was predicted based on measured water retention that is closer to the measured $K(\theta)$ data than a fit to the measured data points. For example, Figures 23 and 24 show that for sites AG-02 and AG-12, predicting K with K_{sat} and θ_{sat} optimized yields curves that are closer to the measured K data than the fit to the measured data points. Over all, the vGM model fits, and in some cases predictions, can lead to reasonable recharge estimates.

In most cases examined in this study, using the Rosetta model resulted in unreasonably high recharge estimates. This is likely due to an over-prediction of K_{sat}, which results in an upward shift of the hydraulic-conductivity curves and thus a higher estimated recharge rate. The database used in the neural network analysis contains a high percentage of near-surface agricultural soils, which are likely to have pronounced structure and therefore higher K_{sat} values than would be expected for the deeper, structureless samples analyzed in this study. It is possible that a measured value of saturated hydraulic conductivity could be used to shift the curve, resulting in more reasonable recharge rates. As an alternative based on principles similar to those of the Rosetta model, multiple linear regression used with a smaller data set comprised of materials more closely related to the samples of interest might provide better estimates of unsaturated hydraulic conductivity for use in recharge estimation.

A combination of the Arya-Paris and vGM models does not lead to either a systematic over-prediction or under-prediction of recharge rates. Though the technique is

highly indirect and the resulting predictions do not always match the measured data well
(Figs. 25 and 26), in some cases it does yield recharge rates that are reasonable, for
example for sites AG-12 and AG-14. Because the coastal plain sands examined in this
study lack significant structure and have relatively narrow particle-size distributions, they
may be more adequately characterized by a texture-based prediction of pore-size
distribution than by a pedotransfer function model like Rosetta. The Rosetta model uses
a database of hydraulic properties from a wide variety of materials including many
agricultural soils. The Arya-Paris model allows the utilization of the highly detailed
particle-size distribution produced by the Coulter LS-230 and sieves, which includes
more than 120 separate size intervals.

Steadiness of Flow

There are complexities that arise in attempting to predict recharge rates at a point
in space as opposed to the watershed scale in humid regions. The assumption of steady
flow below a certain depth is required in applying the Darcian steady-state method. The
Darcian method is generally applied in deep unsaturated zones of the arid southwest.
Steadiness of flow in humid regions has not been as thoroughly investigated. In this
study, two of the sites appeared to have steady flow year-round based on the available
data. Evaluation of what appear to be very small changes in water content over time can
indeed have a significant effect on estimated recharge rates. For site AG-02, which
appears to have little variation in field-water content, the maximum and minimum
recharge values based on a hand interpolation of the data points are 50.5 and 13.2 cm/y,

which occur in spring and summer respectively. This indicates that there may indeed be a seasonal effect that is not apparent upon initial evaluation of water-content profiles. For steady site AG-14, recharge is less than 1 cm/y for all measured water contents. This site has a fine-textured layer at 3.7 m containing 43 percent clay and silt, which may impede downward flow to some degree.

The conceptual model of seasonally steady flow seems to be a more reasonable approach to use in this humid region. For this study, seasons are considered to be four three-month periods. Winter includes December, January, and February, spring includes March, April, and May, summer includes June, July, and August, and fall includes September, October and November. Precipitation is distributed approximately evenly throughout the year; therefore it is the seasonality of ET that may be the primary control on recharge. The main flaw in this approach is the assumption that seasons change over an extremely short period of time, which may or may not be the case in any given year in the New Jersey coastal plain.

Figure 34 shows a comparison of fall recharge estimates determined by all variations of curve fit and prediction techniques as described above for 1996 and 2000 for the sites considered to be seasonally steady. The hand-interpolation technique yields recharge rates of 6.0 cm/yr and 9.5 cm/yr for fall 1996 and 2000, respectively, for site NU-08 and 56.8 cm/yr and 50.0 cm/yr for site AG-12. Because the estimates are similar for fall seasons of different years, they support the idea of seasonality of recharge at some locations. It may be that, for any given season, there is little variation in recharge rate from year to year. For site NU-08, recharge rates determined for summer 2000 and spring
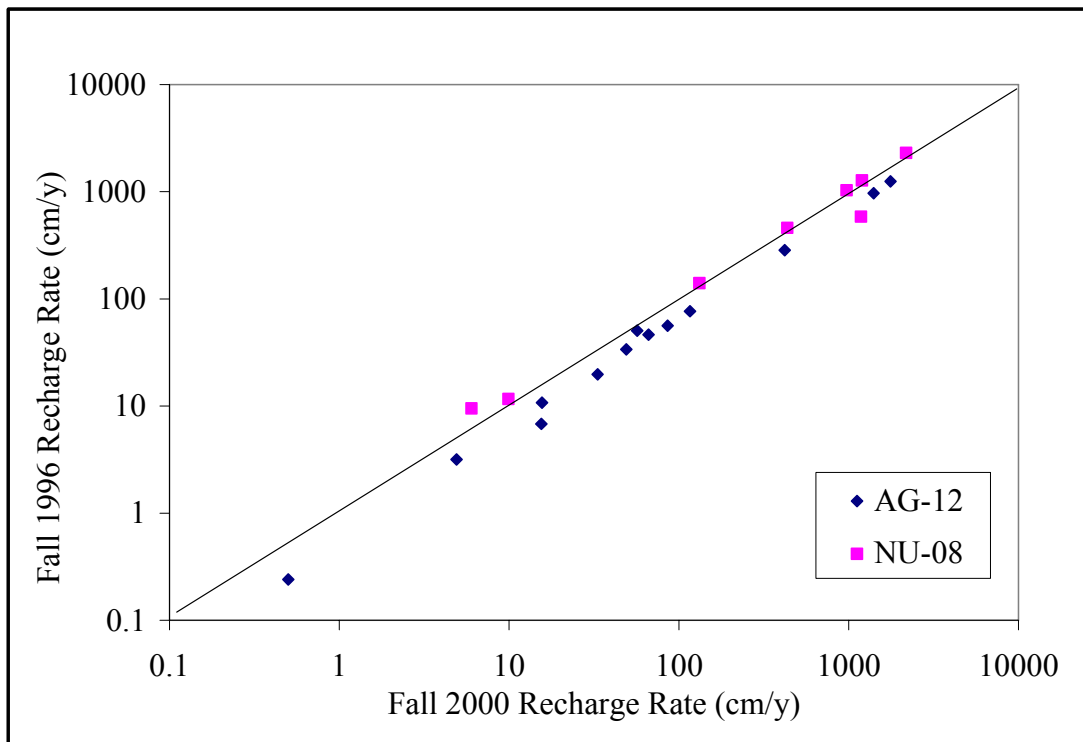
Figure 34. Comparison of recharge rates for the same season (fall) during different years (1996 and 2000) for sites AG-12 and NU-08. Each point represents a recharge rate estimated from a single variation of a hydraulic conductivity curve fit or prediction. The line extending from the origin represents a perfect 1:1 correlation.

2001 are 0 cm/yr and 105.2 cm/yr, respectively (Table 11). The lack of recharge in summer is consistent with high ET. Spring and fall have similar ET conditions, but recharge is much higher in spring, possibly due to high antecedent moisture conditions or a lag in infiltration of winter precipitation. During winter, ET is negligible, allowing infiltration of virtually all precipitation. Site NU-08 appears to have the strongest seasonal influence of all sites and is also the most homogeneous in terms of soil properties. Recharge at this site may occur in sharp seasonal or event-based pulses with little lateral flow. Water contents for AG-12 exhibit seasonality, but recharge rates seem to vary less than at site NU-08 over different seasons, ranging from 58.5 to 78.8 cm/y. This site also exhibits stronger textural contrasts, which may cause recharge to be more diffuse over time. Rather than moving as a pulse of water, as it would through a coarse-textured, homogeneous unsaturated zone, infiltrating water reaches fine-textured layers that control flow to the underlying profile.

Sites AG-15 and NU-01 were inferred to have unsteady flow based on profiles of water content, with fluctuations from 5 to 15 percent in water content compared to fluctuation of 1 to 3 percent for the other sites. Figure 35 shows hydraulic conductivity for these cores with ranges of measured field-water contents indicated by brackets. For site AG-15, recharge values range from around 1 cm/y to more than 600 cm/y indicating the episodic nature of recharge. Site NU-01 varies significantly in water content over time (Fig. 7), but because of the nature of the material, which is fine in texture below about 5 m, and range of water contents, recharge is inferred to be negligible at all times for which there are water-content data.
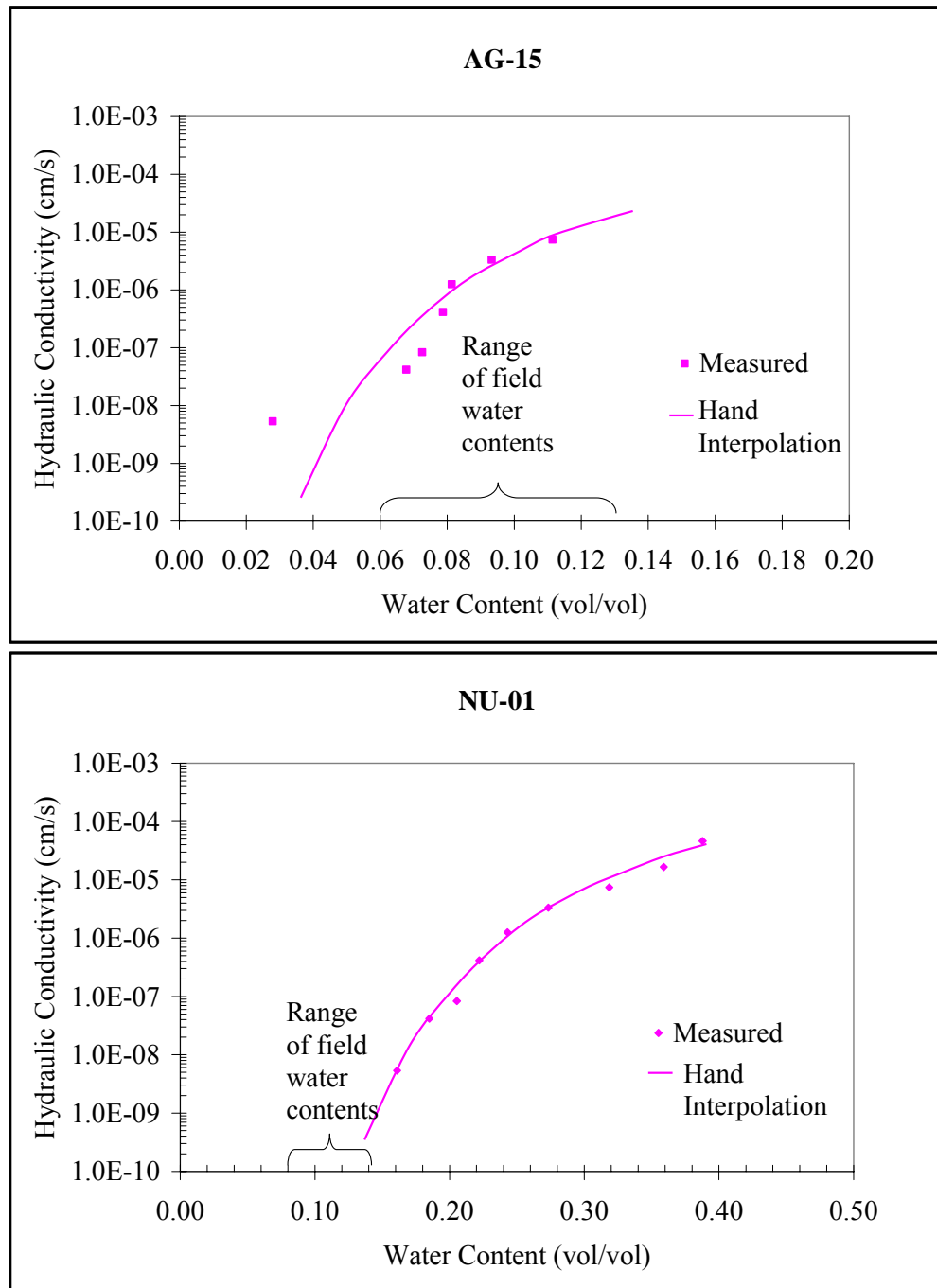
Figure 35. Hand-interpolated hydraulic-conductivity and water-content ranges for sites AG-15 and NU-01. Brackets indicate the range of measured water contents.

Because the field-water-content data are limited, there is a possibility that recharge "pulses" may occur that are not captured in some cases. Water-level data show only seasonal patterns, but there may be fluctuations on a shorter time scale as well that are not apparent due to the lack of temporal data. The analysis here must therefore be viewed as "snapshots" at times for which field-water-content data exist.

The sites examined in this study are clustered near the north and south ends of the study area with one site from each hypothesized flow regime at either end (Fig. 15). Sites such as AG-14, which is inferred to have steady flow, though very low recharge, and AG-12, which has moderate seasonal variability and high recharge, exist within about 5 km of each other. Table 15 summarizes initially hypothesized flow character based on measured field-water contents and flow character based on measured hydraulic-conductivity data.

Table 15. Hypothesized flow character inferred as steady, seasonally steady, or unsteady based on field-water content and sediment character.

Site	Location	Hypothesized nature of recharge based on water content profiles	Sediment character	Nature of flow based on sediment character
AG-02	North	Steady	Upper layers have highest content of fines	Moderately seasonal recharge ranging from 10 to 50 cm/y
NU-08	North	Seasonally steady	Relatively uniform profile, significant gravel	Strongly seasonal recharge ranging from 0 to 100 cm/y
NU-01	North	Unsteady	Fine-textured layer at depth, >30% silt + clay	Negligible recharge
AG-14	South	Steady	Fine-textured layer at depth, , >40% silt + clay	Negligible recharge
AG-12	South	Seasonally steady	Upper layers have highest content of fines	Moderately seasonal recharge ranging from 50-80 cm/y
AG-15	South	Unsteady	Relatively uniform profile, significant gravel	Episodic recharge ranging from 1 to 600 cm/y for unknown periods of time.

It is clear that examination of water content alone is not sufficient to determine flow regime; the nature of the hydraulic properties of the material must also be known and may even be a better indicator of flow regime than water content. Recharge depends not only on climatic variables, but on the hydraulic properties of the material. Those properties can be highly sensitive to very small changes in water content. Sites that appear steady in water content, such as AG-02, may actually have significant variability in recharge over time. Degree of heterogeneity of unsaturated-zone sediment seems to have the largest effect on the recharge regime operating at the local scale.

Comparison of Darcian and Water-table Fluctuation Estimates

Water-level data indicate that recharge is highest in spring and somewhat less, though variable, during the other seasons. Figure 29 shows that, based on water levels, most of the precipitation occurring in spring becomes recharge. The water levels also provide another line of evidence that truly steady flow may not exist at these sites. Well AG-02 shows strong seasonal fluctuations that would not occur under steady-state recharge conditions unless water levels are influenced by phenomena other than recharge through the unsaturated zone, such as stream recharge or discharge. The water-table fluctuations may be showing the overall effect of recharge over a larger portion of the study area, whereas the individual sites vary in amounts and timing of recharge.

CONCLUSION

Because more than 75 percent of public water supply in the coastal-plain region of New Jersey comes from high-capacity ground water production wells, knowing the nature and variability of recharge to the Kirkwood-Cohansey aquifer system is important in the identification of areas potentially susceptible to contamination. It is valuable to be able to identify areas of high recharge where present or future contamination may be an issue, such as in agricultural areas. Upon initial examination of field-water contents measured at six locations within the Glassboro study area in southern New Jersey at various times of the year, it was hypothesized that three possible flow regimes exist in the coastal plain environment: steady, seasonally steady, and unsteady.

This study has shown that, by using measured unsaturated hydraulic properties for Darcian-recharge estimation, recharge is shown to be highly variable over relatively short distances and water contents alone may not provide the information needed to determine steadiness of flow. Very slight variations in measured water content can translate into order-of-magnitude differences in estimated recharge rates if that variation occurs in the region of the hydraulic-conductivity curve where sensitivity to water content is greatest. Degree of heterogeneity in the unsaturated zone, rather than water contents measured over time at a given location, may be a better indication of temporal variations in recharge on a small scale. Sites with greater homogeneity may have more episodic recharge because there is less impediment to downward flow. Significant layering in the

unsaturated zone appears to slow downward flow resulting in a more diffuse, less pulse-like wetting front and therefore less variable recharge over time.

Direct measurement of $K(\theta)$ is recommended for use in the prediction of recharge, although the method of data interpolation is critical. The best interpolation of the data in this study, essentially the one producing the most reasonable recharge estimates, came from hand interpolation and power-law fits to the measured data. Van Genuchten-Mualem fits did well for some cases but not all. Because it is costly and time consuming to measure $K(\theta)$, it is desirable to estimate that function based on more easily measured bulk properties. The use of $K(\theta)$ predicted from the van Genuchten-Mualem and combined Arya-Paris and van Genuchten-Mualem models is not recommended because these techniques yielded an enormous range of recharge rates, with many estimates being unrealistically high, often many times greater than precipitation. The Rosetta model was consistent in over-predicting recharge rates. The Rosetta model could be used with a known K_{sat} value, which would shift the entire curve to yield more reasonable recharge rates. Alternatively, rather than using the Rosetta model to estimate hydraulic properties, it is possible that multiple linear regression used with a smaller data set comprised of materials more similar to those found in the field would provide better data for use in recharge estimation.

There are some limitations to the conclusions drawn in this study due to the nature of the available data. It is probable that some sites have highly episodic flow through the unsaturated zone that was not captured in measured field-water contents. It is recommended to install field instrumentation, such as matric-potential or water-content

sensors, at sites of varying heterogeneity to monitor conditions continuously over some period of time. This would allow for greater confidence in bracketing the range of water contents that occur over time and, consequently, recharge rates estimated from those values.

REFERENCES CITED

Arya, L.M., and Paris, J.F., 1981, A physicoempirical model to predict the soil moisture characteristic from particle-size distribution and bulk density data: Soil Science Society of America Journal, v. 45, p. 1023-1030.

Baehr, A.L., Kauffman, L.J., Perkins, K.S., and Nolan, B.T., 2002, Estimating spatial variability of recharge in southern New Jersey from unsaturated zone measurements: U.S. Geological Survey Water-Resources Investigations Report 02-4288, 31 p.

Brooks, R.H., and Corey, A.T., 1964, Hydraulic properties of porous media: Colorado State University Hydrology Paper No. 3, 27 p.

Charles, E.G., Storck, D. A., and Clawges, R. M., 2001, Hydrology of the unconfined aquifer system, Maurice River area: Maurice and Cohansey River basins, New Jersey, 1994-95: U.S. Geological Survey Water-Resources Investigations Report 01-4229, 5 p.

Conca, J.L., and Wright, J.V., 1998, The UFA method for rapid, direct measurements of unsaturated soil transport: Australian Journal of Soil Research, v. 36, p. 291-315.

dos Santos, A.G. Jr., and Young, E.G., 1969, A study of the specific yield in land-drainage situations: Journal of Hydrology, v. 8, p. 59-81.

Duke, H.R., 1972, Capillary properties of soils—influence upon specific yield: Transactions of the American Society of Agricultural Engineers, v. 15, p. 688-691.

Flint, A.L., and Flint, L.E, 2002a, Particle density, *in* Dane, J.H., and Topp, G.C., eds., Methods of soil analysis, part 4—physical methods: Madison, Wisconsin, Soil Science Society of America Book Series No. 5, p. 229-240.

Flint, L.E., and Flint, A.L., 2002b, Porosity, *in* Dane, J.H., and Topp, G.C., eds., Methods of soil analysis, part 4—physical methods: Madison, Wisconsin, Soil Science Society of America Book Series No. 5, p. 241-253.

Gardner, W.H., 1986, Water content, *in* Klute, A., ed., Methods of soil analysis, part 1—physical and minerological methods: Madison, Wisconsin, Soil Science Society of America Book Series No. 5, p. 503-507.

Gee, G.W., and Or, D., 2002, Particle-size analysis, *in* Dane, J.H., and Topp, G.C., eds., Methods of soil analysis, part 4—physical methods: Madison, Wisconsin, Soil Science Society of America Book Series No. 5, p. 255-293.

Healy, R.W., 1990, Simulation of solute transport in variably saturated porous media with supplemental information on modifications to the U.S. Geological Survey's computer program VS2DT: U.S. Geological Survey Water-Resources Investigations Report 90-4025, 125 p.

Healy, R.W., and Cook, P.G., 2002, Using groundwater levels to estimate recharge: Hydrogeology Journal, v. 10, p. 91-109.

Hsieh, P.A., Wingle, W., and Healy, R.W., 1999, VS2DTI—a graphical user interface for the variably saturated flow and transport computer program VS2DT: U.S. Geological Survey Water-Resources Investigations Report 99-4130, 13 p.

Johnson, A.I., 1967, Specific yeild—compilation of specific yields for various materials: U.S. Geological Survey Water Supply Paper 1662D, 74 p.

Johnson, M.L., and Charles, E.G., 1997, Hydrology of the unconfined aquifer system, Salem River area: Salem River and Racoon, Oldmans, Alloway, and Stow Creek basins, New Jersey 1993-94: U.S. Geological Survey Water-Resources Investigations Report 96-4195, 5 p.

Johnson, M.L., and Watt, M. K., 1994, Hydrology of the unconfined aquifer system, Mullica River basin, New Jersey 1991-92: U.S. Geological Survey Water-Resources Investigations Report 94-4234, 6 p.

Jury, W.A., Gardner, W.R., and Gardner, W.H., 1991, Soil physics (fifth edition): New York, New York, John Wiley and Sons, Inc., 328 p.

Lappala, E.G., Healy, R.W., and Weeks, E.P., 1983, Documentation of the computer program VS2D to solve the equations of fluid flow in variably saturated porous media: U.S. Geological Survey Water-Resources Investigations Report 83-4099, 184 p.

Mualem, Y., 1976, A new model for predicting the hydraulic conductivity of unsaturated porous media: Water Resources Research, v. 12, p. 513-522.

Nimmo, J.R., and Mello, K.A., 1991, Centrifugal techniques for measuring saturated hydraulic conductivity: Water Resources Research, v. 27, p. 1263-1269.

Nimmo, J. R., Perkins, K.S., and Lewis, A.M., 2002, Steady-state centrifuge, *in* Dane, J.H., and Topp, G.C., eds., Methods of soil analysis, part 4—physical methods:

Madison, Wisconsin, Soil Science Society of America Book Series No. 5, p. 903-916.

Nimmo, J.R., Rubin, J., and Hammermeister, D.P., 1987, Unsaturated flow in a centrifugal field: measurement of hydraulic conductivity and testing of Darcy's law: Water Resources Research, v. 23, p. 124-134.

Nimmo, J.R., Stonestrom, D.A., and Akstin, K.C., 1994, The Feasibility of recharge rate determinations using the steady-state centrifuge method: Soil Science Society of America Journal, v. 58, p. 49-56.

Pachepsky, Y.A., Timlin, D., and Varallyay, G., 1996, Artificial neural networks to estimate soil water retention from easily measurable data: Soil Science Society of America Journal, v. 60, p. 727-733.

Richards, L.A., 1931, Capillary conduction of liquids through porous media: Physics, v. 1, p. 318-333.

Sammis, T.W., Evans, D.D., and Warrick, A.W., 1980, Comparison of methods to estimate deep percolation rates: Water Resources Bulletin, v. 18, no. 3, p. 466-470.

Schaap, M.G., and Leij, F.J., 1998, Database related accuracy and uncertainty of pedotransfer functions: Soil Science, v. 163, p. 765-779.

Schaap, M.G., Leij, F.J., and van Genuchten, M.Th., 1998, Neural network analysis for hierarchical prediction of soil water retention and saturated hydraulic conductivity: Soil Science Society of America Journal, v. 62, p. 847-855.

Schaap, M.G., Leij F.J. and van Genuchten M.Th., 1999, A bootstrap-neural network approach to predict soil hydraulic parameters, *in* van Genuchten, M.Th., Leij, F.J., and Wu, L., eds., Procedings of the international. Workshop on characterization and measurements of the hydraulic properties of unsaturated porous media: University of California, Riverside, CA, p. 1237-1250.

Soil Survey Staff, 1975, Soil taxonomy: A basic system of soil classification for making and interpreting soil surveys: USDA-SCS Agriculture Handbook n. 436, U.S. Government Printing Office, Washington, DC, 754 p.

Thornthwaite, C.R., and Mather, J.R., 1957, Instructions and tables for computing potential evapotranspiration and the water balance: Publications in Climatology, v. 10, p. 185-311.

U.S. Department of Agriculture, 2001, Soil Salinity Laboratory: http://www.ussl.ars.usda.gov/models/models.htm, information retrieved 4/2001.

U.S. Geological Survey, 1998, Major aquifers in New Jersey:
http://nj.water.usgs.gov/gw/aquifer.html, information retrieved 11/2001.

U.S. Geological Survey, 2003, Groundwater information for New Jersey Counties:
http://nj.usgs.gov/gw/county_imagemap.html, information retrieved 1/2003.

van Genuchten, M.Th., 1980, A closed-form equation for predicting the hydraulic
conductivity of unsaturated soils: Soil Science Society of America Journal, v. 44,
p. 892-898.

van Genuchten, M.Th., Leij, F.J., and Yates, S.R., 1991, The RETC code for quantifying
the hydraulic functions of unsaturated soils: U.S. Environmental Protection
Agency Report EPA/600/2- 91/065, 85 p.

Watt, M. K., and Johnson, M. L., 1992, Water resources of the unconfined aquifer system
of the Great Egg Harbor River Basin, New Jersey, 1989-1990: U.S. Geological
Survey Water-Resources Investigation Report 91-4126, 5 p.

Watt, M. K., Johnson, M. L., and Lacombe, P.J., 1994, Hydrology of the unconfined
aquifer system, Toms River, Metedeconk River, and Kettle Creek basins, New
Jersey, 1987-90: U.S. Geological Survey Water-Resources Investigation Report
93-4110, 5 p.

Young, M.H, and Sisson, J.B, 2002, Tensiometry, *in* Dane, J.H., and Topp, G.C., eds.,
Methods of soil analysis, part 4—physical methods: Madison, Wisconsin, Soil
Science Society of America Book Series No. 5, p. 575-606.

Zapecza, O. S., 1989, Hydrologic framework of the New Jersey coastal plain: U.S.
Geological Survey Professional Paper 1404-B, 49 p.